



Understanding a protein fold: The physics, chemistry, and biology of α -helical coiled coils

Received for publication, January 3, 2023, and in revised form, February 25, 2023 Published, Papers in Press, March 5, 2023,
<https://doi.org/10.1016/j.jbc.2023.104579>

Derek N. Woolfson^{1,2,3,4,*}

From the ¹School of Chemistry, University of Bristol, Bristol, United Kingdom; ²School of Biochemistry, University of Bristol, Medical Sciences Building, University Walk, Bristol, United Kingdom; ³BrisEngBio, School of Chemistry, and ⁴Max Planck-Bristol Centre for Minimal Biology, University of Bristol, Bristol, United Kingdom

Reviewed by members of the JBC Editorial Board. Edited by Wolfgang Peti

Protein science is being transformed by powerful computational methods for structure prediction and design: AlphaFold2 can predict many natural protein structures from sequence, and other AI methods are enabling the *de novo* design of new structures. This raises a question: how much do we understand the underlying sequence-to-structure/function relationships being captured by these methods? This perspective presents our current understanding of one class of protein assembly, the α -helical coiled coils. At first sight, these are straightforward: sequence repeats of hydrophobic (*h*) and polar (*p*) residues, (*hpph*_n), direct the folding and assembly of amphipathic α helices into bundles. However, many different bundles are possible: they can have two or more helices (different oligomers); the helices can have parallel, antiparallel, or mixed arrangements (different topologies); and the helical sequences can be the same (homomers) or different (heteromers). Thus, sequence-to-structure relationships must be present within the *hpph*_n repeats to distinguish these states. I discuss the current understanding of this problem at three levels: first, *physics* gives a parametric framework to generate the many possible coiled-coil backbone structures. Second, *chemistry* provides a means to explore and deliver sequence-to-structure relationships. Third, *biology* shows how coiled coils are adapted and functionalized in nature, inspiring applications of coiled coils in synthetic biology. I argue that the chemistry is largely understood; the physics is partly solved, though the considerable challenge of predicting even relative stabilities of different coiled-coil states remains; but there is much more to explore in the biology and synthetic biology of coiled coils.

As a graduate student in the late 1980s, I was drawn to the challenge of the protein-folding problem and to using protein design as a means of testing our understanding of protein structure and folding. Even then, we suspected that solutions to these problems would come through bioinformatics. However, we did not realize how long it would take for solutions to come or the form that they would take in terms of combining big data, large computer power, and artificial intelligence, specifically, machine learning. Of course, I refer to

the recent successes AlphaFold2 and RoseTTAFold in predicting protein structure from sequence alone (1–4). Like many, when I look at an AlphaFold2 model for a complex protein assembly, I am awestruck by the structural solutions that it finds. However, while AlphaFold2 and RoseTTAFold provide solutions to the protein-folding problem—and, to be sure, these and other methods will improve to provide models for ever-more complex protein structures and assemblies—they are just that, *solutions*. In themselves, they do not necessarily, at least not at present, provide an *understanding* of the physics and chemistry that drives and directs protein folding and assembly, which, in turn, are responsible for protein function.

Back in the 1980s and 1990s, it was the desire to understand protein folding that drove interest in the field; it was not just to find solutions to the problem *per se*. In short, we wanted to understand the physico-chemical principles that underpin protein structure, folding, assembly, and stability. In other words, we sought to decipher the underlying sequence-to-structure relationships for these properties. This perspective is about how far we have progressed in understanding protein folding and design in these terms. Well, at least for one particular protein structure—the α -helical coiled coil. At first sight, this is a relatively straightforward peptide and protein assembly in which two or more α -helical chains wrap around each other to form supercoiled or rope-like structures, Figure 1.

At that time, coiled-coil-forming leucine-zipper peptides, Figure 1A, became models for protein folding and design (5–7). I was drawn to the folding and design of leucine zippers as a post-doc with Tom Alber in the early 1990s. This was because of the apparent simplicity of these coiled coils and the thought that *unless we could understand such simple protein folds and assemblies, we would have no hope with more complex globular proteins*. Therefore, I adopted coiled coils as a model for developing an understanding of sequence-to-structure relationships in proteins. An aim of this perspective is to capture some of that journey, which has been contributed to by many scientists in many groups over the past few decades. However, it is not a *complete* review of coiled-coil structure, biology, or even design. Such an article would be redundant because many excellent reviews are already available (8–14), as are others covering newer topics such as the applications of natural and

* For correspondence: Derek N. Woolfson, D.N.Woolfson@bristol.ac.uk.



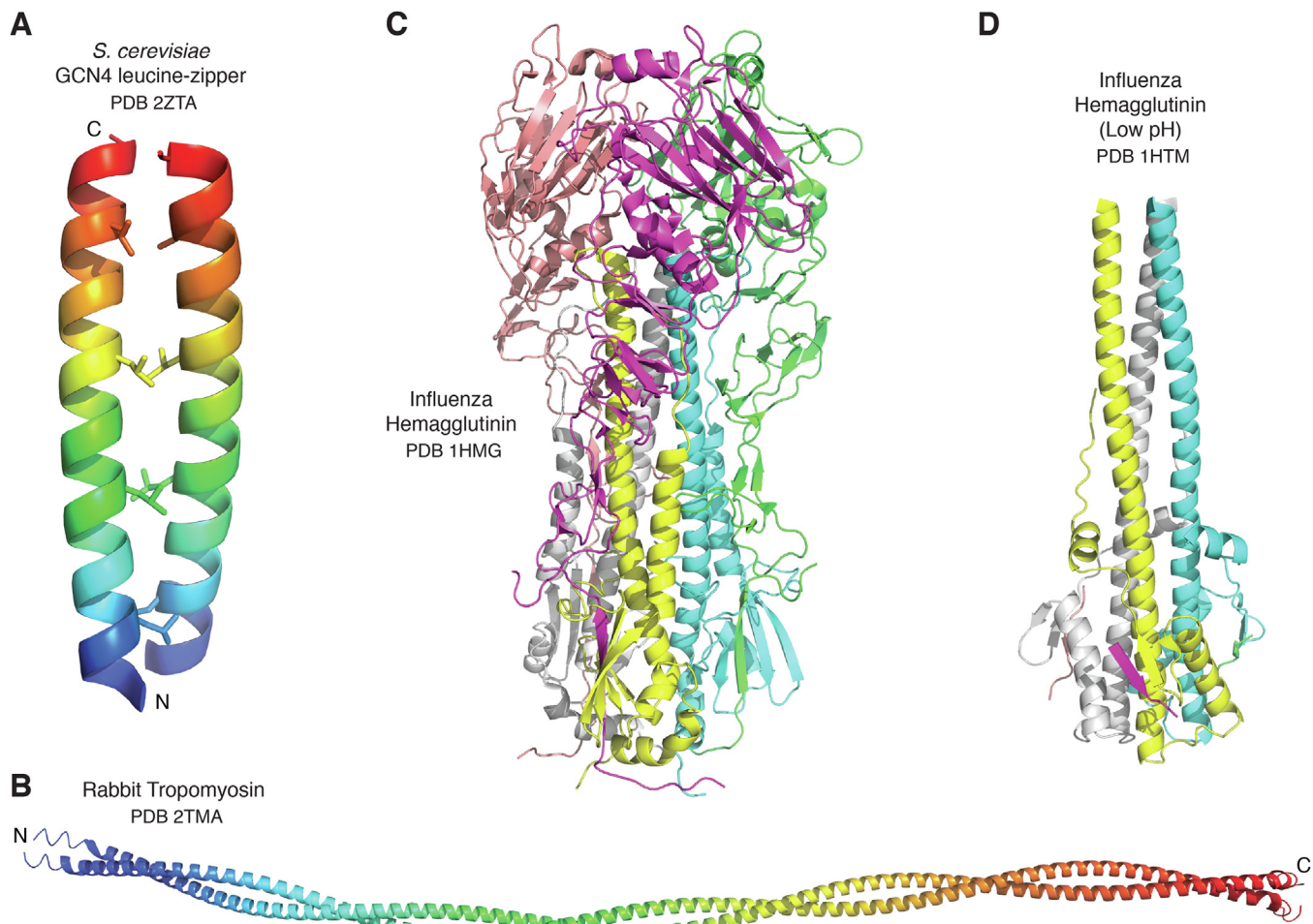


Figure 1. Early coiled-coil structures. *A*, 1.8 Å atomic-resolution structure of the leucine-zipper peptide from *Saccharomyces cerevisiae* (2zta (6)). An NMR structure for a similar peptide was determined in the same year (1zta (288)). *B*, 15 Å model of rabbit tropomyosin (2tma (43)), later refined to 7 Å (1c1g (44)). *C*, 3 Å resolution structure of influenza hemagglutinin (PDB id 1hmg (45)), later refined as 2hmg (289)). *D*, 2.5 Å structure of a fragment influenza hemagglutinin at a low pH of (1htm (46)). Coloring schemes: for *A* and *B*, the chains are colored by chainbow from their *N* termini (blue) through to their *C* termini (red); for *C* and *D*, the protomers of each trimer are colored differently, with the central coiled-coil chains in gray, yellow, and cyan. The images were generated using PyMOL (pymol.org). PDB, Protein Data Bank.

designed coiled coils in biotechnology and synthetic biology (15–18). Instead, I want to give some sense of three things: first, of the journey and the joy of discovery, which have led to our current understanding of this relatively straightforward protein structure; second, that in some respects—for instance, the physics and chemistry of coiled-coil folding and assembly—our understanding is complete or very near to it; and third, despite this understanding, we still have much to learn, particularly on the biology of coiled coils.

This article is my perspective on the amassed understanding of coiled-coil proteins. Indeed, it closes some of my own research questions; namely, *what are the sequence-to-structure relationships that govern coiled-coil folding and assembly, and how do these allow us to design de novo coiled coils with confidence?* However, as some research chapters close, others open. For coiled-coil research, new challenges include the following: achieving fully quantitative (free-energy) predictions for coiled-coil structure, stability, and partner selection; gaining a deeper understanding of coiled-coil dynamics and plasticity and how

this relates to coiled-coil function. And, as one of the best understood protein folds, how can *de novo* coiled-coil peptides and proteins be used in biotechnology and synthetic biology to address real-world applications, for instance, in health and the environment. I am certain that the methods, principles, and understanding that have been developed over the past few decades will provide a foundation for these and other endeavors. And to come full circle, it is clear that new artificial intelligence/machine learning-based methods for protein-structure prediction will contribute here. Indeed, I see these tools as fantastic hypothesis generators for structural molecular and cell biology, including for processes that involve relatively simple, but adaptable and versatile coiled coils.

The physics of coiled coils: A firm foundation for developing understanding

For more complete historical perspectives on the conceptual origins of α -helical coiled coils, please see reviews by Squire and Parry and by Lupas et al. (19–21).

The coiled coil came out of physics: Francis Crick's description of the coiled coil, as he first named it, is mathematical (22, 23). Moreover, at that time in the early 1950s, there was little experimental data or confirmed details for any protein structure. So, what followed—namely, the first description of any protein structure, the concepts of helical nets and knobs-into-holes (KIH) packing, heptad repeats, and what we now refer to as the Crick Equations—was extremely insightful. Incidentally, Crick published this work in the same year that he and James Watson proposed the double helix for the structure of DNA (24).

Crick started with Linus Pauling's α helix and its regularity (Fig. 2A) (25). As a consequence of steric constraints in polypeptide chains—as later formalized by Ramachandran in his famous plot (26, 27)—the α helix has precisely 3.6 residues per turn (Fig. 2A). Crick reasoned that two or more such helices could interact tightly *via* seams of interacting side chains spaced three and four residues apart along polypeptide chains—*i.e.*, with an average spacing of 3.5 residues—to match the 3.6 residues per turn as closely as possible. Now, we annotate these repeats **abcdefg** with the key interacting side chains falling at the **a** and **d** sites. Crick visualized this with helical-net diagrams (Fig. 2B). Highlighting the 3,4 spacing on one of these reveals the seam as the line of connected diamond shapes. Two such seams can interlace to bring the helices into intimate contact (Fig. 2C): the diamonds on one helix form 'holes' into which side chains from the other helix can slot. In this way, Crick coined the terms 'heptad repeat' (from the Greek for seven) and KIH packing for these sequence and structural features, respectively. These are now the hallmarks for coiled-coil peptides and proteins, and they provide a firm basis for understanding them.

The term 'coiled coil' is a consequence of these sequence patterns and the structural packing. This is because 3.5 is less than 3.6. As a result, on a helical net, the seam slants to the left (Fig. 2B). Thus, for two nets to interlace requires one to be offset at an angle to the other (Fig. 2C). In a 3D α helix, the seam precesses around the surface of the helix with the opposite sense to the handedness of the helix. Thus, for two α helices to maintain contact, they must wrap around each other like the strands of a rope. As α helices made from L-amino acids are right handed, heptad-based coiled coils are left-handed ropes. This overall assembly—which is a quaternary structure and not a tertiary structure—is also helical. Strictly, it is a superhelix. This is why Crick called the envisaged structures coiled coils; "coils" refers to the α helices, and "coiled" refers to the superhelix.

From Pauling's α -helical parameters—3.6 residues per turn and a rise per residues of 1.5 Å—Crick predicted that the crossing angle between the two helices would be $\approx 20^\circ$, which gives a superhelical pitch of ≈ 126 residues or ≈ 186 Å (Box 1). (Note: these values correspond to those observed in experimentally determined coiled coils (28, 29)). This is formalized in the Crick Equations. Thus, the coiled coil is inherently parametric, which makes it physics, predictable, modelable and, as, we will see, ultimately designable (28). Indeed, this formalism has led to a swathe of coiled-coil modeling and design

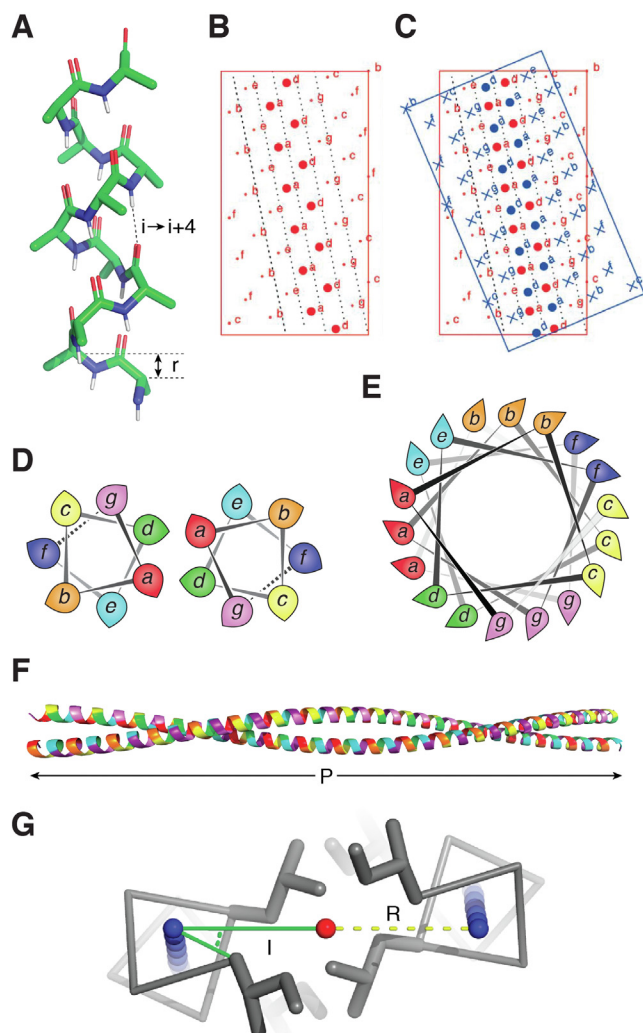


Figure 2. α -Helix and coiled-coil geometry. A, the α helix has a rise per residue (r) of 1.5 Å, 3.6 residues per helical turn, a backbone radius of 2.3 Å, and is stabilized by i_{CO} to $i + 4_{\text{NH}}$ hydrogen bonds. B, in Crick's helical nets, the positions of the Ca atoms of an α helix, are projected as points onto a 2D plot (red). Here, the heptad repeats, **abcdefg**, are annotated onto the points with the **a** and **d** sites emphasized as discs. C, overlay of the helical net from B and a second net in blue with crosses and discs for the Ca positions. Note how the **a** and **d** sites interdigitate, which leads naturally to the helices packing in a slanted rather than straight manner. In turn, this causes the α helices to wrap or supercoil around each other (see panel F). D, helical-wheel diagrams where heptad repeats, **abcdefg**, for a parallel, dimeric coiled coil are projected onto circles representing backbones of each helix viewed from one end. The **a → g** register is rainbow colored, *i.e.* by the visible spectrum, red → violet. Note that these wheels are idealized with 3.6 residues per turn to make the seven residues span exactly two turns; they are plotted in 'superhelical space'. This is opposed to the true α helix, which repeats every 18-residue or five turns, as depicted in panel (E). F and G, Crick's parameterization of coiled coils illustrating its three main parameters: coiled-coil radius (R), interface (or Crick) angle (I), and pitch (P). These and the 3.6 residues per turn of the α helix are the only parameters needed to define any regular α -helical coiled-coil assembly. The structure shown in panel (F) was built using CCBUILDER2.0 (36). Panels A, F, and G were generated in PyMOL (pymol.org). Panels B and C are adapted from Walsh and Woolfson (2003) (96) with permission.

programs (28–36). Several of these are accessible and easy-to-use computational tools on the internet (Box 2). Some allow coiled-coil backbones to be built quickly and accurately (28, 31), and others allow full atomistic modeling of coiled coils including side chains (29, 33, 35, 36). Furthermore, there are tools for assessing the quality of such models and experimental

Box 1. From α -helical to coiled-coil parameters

The following exercise can be done by considering projections of the α helix as helical nets or helical wheels.

First, I need to dispel a key misconception made by students and professors alike. Pauling's α helix has 3.6 residues per turn with a very low tolerance of variation (29); indeed, this is one of the few fixed physical constants in biology (52). This is because the energy well for the α helix is narrow and deep (53), and small deviations from α -helical parameters incur large energy penalties. Indeed, the nearby 3_{10} and π helices are rare in protein structures and difficult to design (52). As a result, the α helix does not somehow collapse to 3.5 residues per turn in coiled coils. If it did, we would not have coiled coils: the average sequence repeat of 3.5 and a helical repeat of 3.5 would match, and the helices would pack straight and not wrap around each other. I suspect that the convenience of 7-residue helical wheels (Fig. 2D) rather than the more accurate 18-residues helical wheels (Fig. 2E) has contributed to this misconception. Crick's helical nets are a more faithful mapping of an α -helical surface in 2D (Fig. 2B).

With the C α atoms of an α helix projected on an 18-residue helical wheel, successive residues are separated by 100°. Thus, the seven residues of a heptad repeat would span out 700°. This is 20° short of two full turns ($2 \times 360^\circ = 720^\circ$ and 7.2 residues) of the α helix. 20° goes into 360° 18 times. Therefore, 18 heptad repeats are required for the interacting seam to make one complete revolution of a helix and to bring the helices back into sync. This defines the pitch of the coiled coil. Hence, the pitch is $18 \times 7 = 126$ residues. Given that the α helix has a rise per residue of 1.5 Å, these would span 189 Å of a straight α helix. However, each α helix is inclined by $\approx 10^\circ$ relative to the superhelical axis. Therefore, the rise per residue along this coiled-coil axis is $1.5 \times \cos(10^\circ) = 1.48$ Å, and the ideal superhelical pitch is ≈ 186 Å (Fig. 2F). In addition to the rise per residue and the coiled-coil pitch, just two other parameters are needed to define and generate regular coiled-coil backbones. These are the radius of the coiled coil and the interface or Crick angle, Figure 2G.

Finally for this Box, we should also credit Pauling. Crick considered only 7-residue repeats. However, Pauling et al. considered other repeats in α -helical conformations, specifically, those with 11, 15, and 18 residues (25, 54). Along with 7-residue repeats, these are compatible with combinations of 3- and 4-residue spacings; namely, 3-4, 3-4-4, 3-4-4-4, and 3-4-3-4-4, respectively. However, they have different average spacings between the interacting residues of 3.5, 3.67, 3.75, and 3.6, respectively. As the α -helical structural repeat is fixed at 3.6 residues per turn, when these repeats are realized in packed coiled coils, they lead to different superhelical twists. These can also be calculated using the considerations laid out above. They result in further left-handed, some right-handed, and even "straight" coiled coils (19, 55–58).

structures parametrically and energetically (32, 37–39). This has made coiled-coil modeling, engineering, and design accessible to nonexperts, which is a significant advance. In turn, this has enabled the exploration of coiled-coil assemblies beyond the confines of natural proteins (34, 40).

Experimental realization of Crick's model

Crick's formalism has been confirmed by numerous experiments and analyses over the past 4 to 5 decades (20, 41), as illustrated by the following. In 1972, Sodek et al. reported the partial sequence of rabbit tropomyosin (42), which was anticipated to be an extended dimeric coiled coil. This showed clear and unbroken repeats with mainly hydrophobic residues spaced alternately three and four residues apart; in retrospect, these are unmistakable as heptad repeats. Later, low-resolution 15 Å (43) and 7 Å (44) structures from EM and X-ray diffraction revealed a supercoiled pair of α helices, Figure 1B. Wilson, Skehel, and Wiley published the first high-resolution structure of a coiled coil in 1981 for the trimeric influenza hemagglutinin (45), Figure 1C. The hemagglutinin story became more interesting as it unraveled; for example, revealing

Box 2. Tools and resources for predicting, building, analyzing, and visualizing coiled-coil structures**Prediction**

Several tools for predicting coiled-coil structure from sequence are brought together and implemented at Andrei Lupas's Max Planck Institute Bioinformatics Toolkit (59) (<https://toolkit.tuebingen.mpg.de/>). These include the following: Lupas's original COILS program (60) (now PCOIL), DeepCoil (61), and MARCOIL (62). Regarding predicting oligomeric states from sequence, in light of recent advances in coiled-coil design and protein-structure prediction, generally, there is considerable room for improvement here. However, the following are currently available: LOGICOIL (63) (<http://coiledcoils.chm.bris.ac.uk/LOGICOIL/>) and Multicoil2 (64) (<http://cb.csail.mit.edu/cb/multicoil2/cgi-bin/multicoil2.cgi>). AlphaFold2 (3) also predicts coiled-coil regions, though this has to be done using "multimer" mode, and an evaluation of AlphaFold2 predictions against the CC+ database (see below) for instance needs to be done (<https://colab.research.google.com/github/deepmind/alphafold/blob/main/notebooks/AlphaFold.ipynb>).

Model building

Useful online tools for modeling coiled coils include the following: CCBUILDER (29) and CCBUILDER2 (36) for real-time all-atom modeling of coiled coils (<http://coiledcoils.chm.bris.ac.uk/ccbuilder2/builder>). These web-based apps use ISAMBARD (35) as a backend, which can also be run using Python-based scripts for more detailed and accurate modeling of parametric biomolecular structures (<https://github.com/isambard-uob>). Coiled-coil Crick Parametrization (CCCP, (28)) from the Grigoryan lab builds coiled-coil backbones (<https://grigoryanlab.org/cccc>). Coiled-coil Protein Origami Design platform (CoCoPOD, (65)) designs amino-acid sequences and builds 3D models for arbitrary polyhedral meshes constructed from single chain polypeptides (https://github.com/NIC-SBI/CC_protein_origami). And Rosetta has a MakeBundle mover (https://www.rosettacommons.org/docs/latest/scripting_documentation/RosettaScripts/Movers/movers_pages/MakeBundleMover).

Analyses of structures

The following programs analyze coiled-coil structures from Protein Data Bank (PDB) files. SOCKET (37) and Socket2 (39) identify the signature KIH interactions and calculate coiled-coil parameters more generally (<http://coiledcoils.chm.bris.ac.uk/socket2/home.html>). TWISTER (38) determines coiled-coil parameters (<https://pharm.kuleuven.be/apps/biocryst/twister.php>). And samCC (32) measures local parameters of (a)symmetric, parallel, and antiparallel four-helical bundles (<https://toolkit.tuebingen.mpg.de/tools/samcc>).

Databases and related resources

Finally, the following databases helpfully collect together and categorize coiled-coil structures from the RCSB PDB (66): the searchable CC+ database (50) generated from the PDB using SOCKET (http://coiledcoils.chm.bris.ac.uk/ccplus/search/dynamic_interface); the Periodic Table of Coiled Coils (67) (http://coiledcoils.chm.bris.ac.uk/ccplus/search/periodic_table); the Atlas of Coiled Coils that followed (68) (<http://coiledcoils.chm.bris.ac.uk/atlas/index>); and CCdb generated from the PDB using samCC-Turbo (69) (<https://lbs.cent.uw.edu.pl/ccdb>).

a spring-loaded switch to a longer trimeric CC leading to virus-host membrane fusion, Figure 1D (46, 47), and targets for drug design (48, 49). In 1991, O'Shea, Alber, and Kim determined the first atomic-resolution coiled-coil structure for the leucine-zipper peptide of the yeast transcriptional activator GCN4 (6), Figure 1A. This showed both the supercoiling of two parallel α helices and intimate interdigititation of side chains predicted by Crick. Since then, many thousands of coiled-coil structures have been resolved, ushering in efforts to automate their identification, analysis, and categorization

(Box 2). With some tweaks, the main tenets of Crick's model are evident and validated by these structures and analyses (19, 20, 37, 50).

In summary, Pauling gave us the α helix and, using this, Crick gave us the coiled coil with its sequence signature of 3,4 or heptad repeats and its structural signature of the KIH interactions. Indeed, I contend that for an α -helical assembly to be considered a coiled coil, it has to have a recognizable sequence pattern and KIH interactions. Moreover, as described in the next section, the simplicity and reliability of Crick's model allows protein designers to make reliable coiled-coil models *in vivo* (*i.e.*, simply by drawing) or *in silico*, build sequences to fit these, realize them experimentally, and confirm that the models match the experimental structures with atomic accuracy (51).

So, is the physics of the coiled coil solved? In a word, no. This is because, despite our abilities to predict, build, and design coiled-coil structures, we cannot predict *ab initio* the free energy of folding and stability of a coiled-coil sequence or the relative free energies between alternate coiled-coil states that it might form. I return to these gaps and challenges later. Nonetheless, and as we will see in the next section, we have sufficient rules of thumb (*i.e.*, *chemistry*) to understand the assembly of natural coiled coils and to deliver an impressive array of these *de novo* designed assemblies.

The chemistry of coiled coils: Rules for coiled-coil assembly and design

The foregoing section skipped an important detail on the precise nature of the interacting side chains separated by three and four residues in heptad repeats. This was because Crick's model is pure physics and agnostic of detailed side-chain chemistry. Arguably, however, we understand the chemistry of α -helical coiled coils—*i.e.*, their sequence-to-structure relationships—better than for any other protein structure. Indeed, I contend that we are close to a complete chemical understanding of coiled-coil structure and assembly, and others agree (51, 69, 70). This section describes our current understanding of this chemistry.

The primary interacting side chains in coiled coils are assumed to be hydrophobic. That is, the 3,4 or heptad repeats are traditionally considered as ***hphphpp*** repeats, where ***h*** and ***p*** are hydrophobic and polar side chains, respectively. When folded, these form amphipathic α helices with a hydrophobic seam and a polar face, Figure 3A. In water, driven by the hydrophobic effect, two or more such helices assemble to bury their hydrophobic seams and form a hydrophobic core, Figure 3B. However, these cores are very different from those of globular proteins (6, 19, 37, 45, 50). In coiled coils, the KIH packing is tight and intimate; whereas, in globular proteins, the side chains pack more loosely (71). This has important consequences: coiled coils can achieve high stability and specificity from relatively short stretches of sequence. Indeed, the ≈30-residue leucine-zipper domains are half the size of even the smallest recognized globular proteins and on a par with so-called miniproteins, which are a niche type of protein (72).

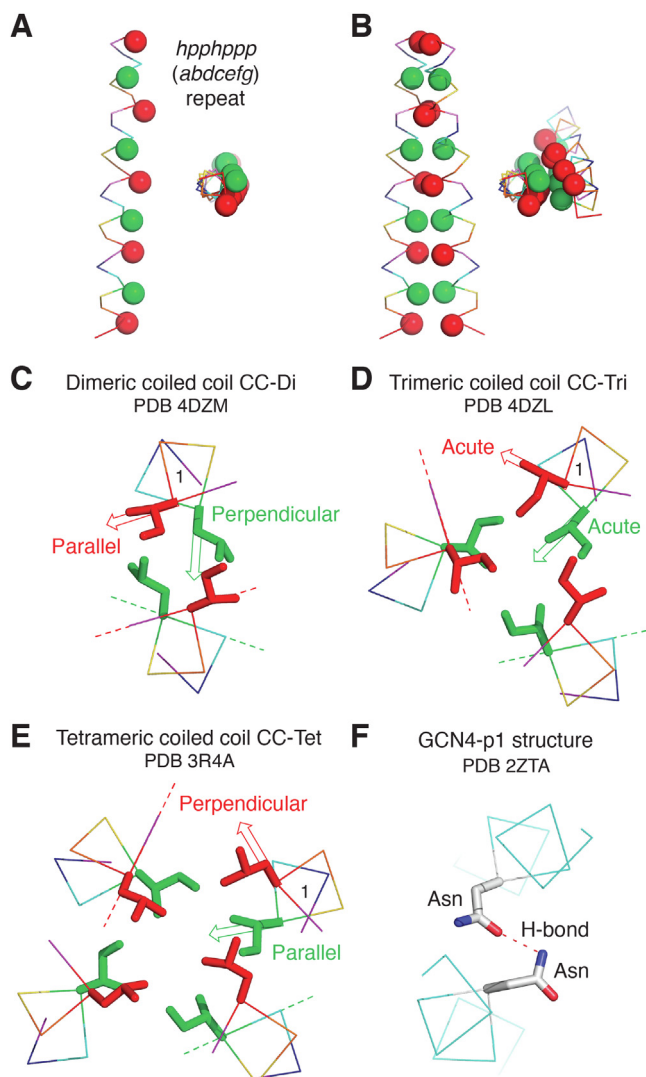


Figure 3. Amphipathic α helices and how they pack in coiled coils. A, orthogonal views of an ***hphphpp*** (***abcdefg***) repeat superimposed on an α -helical backbone with ***h*** residues picked out as spheres and the ***a*** and ***d*** sites colored red and green, respectively. B, two such amphipathic helices assembled via their hydrophobic faces with the same coloring as in panel A. C–E, slices through the X-ray crystal structures of dimeric (C, CC-Di, PDB id 4dzm), trimeric (D, CC-Tri, PDB id 4dzl), and tetrameric (E, pLI, PDB id 3r4a) *de novo*-designed coiled coils (89, 100). The backbones are shown as Ca traces with rainbow coloring for the ***abcdefg*** sites, and the side chains at the ***a*** and ***d*** sites depicted in red and green sticks, respectively. The assemblies were oriented by aligning helices labeled '1' in PyMol. This highlights the different types of knobs-into-holes (KIH) packing at the ***a*** and ***d*** sites in each assembly. The directions of the knobs are shown with open red and green arrows, and the bases of the corresponding holes are shown as broken red and green lines on the partnering helices. There are three types of KIH packing: in **perpendicular packing**, the Ca-C β bond vector of the knob residue points directly at the base of the hole, defined by a Ca-Ca vector on the partner helix; in **parallel packing**, the Ca-C β bond vector of the knob aligns parallel with the base of the hole; and in **acute packing**, the arrangement lies between these two extremes. F, slice through the central heptad of the GCN4-p1 structure (PDB id 2zta) showing an Asn:Asn side-chain hydrogen bond. Images made in PyMol (pymol.org). PDB, Protein Data Bank.

There is another more subtle consequence that I develop below: KIH packing discriminates between ***h***-type residues such that they are not all equal in terms of coiled-coil folding, assembly, and stabilization. That is all chemistry.

The aim of this section is three-fold: first, to demonstrate that there is much more to coiled-coil sequences than simple **hp** patterns and that there are clear sequence-to-structure relationships for coiled-coil folding, assembly, stability, and specificity; second, to show that these relationships are more than simple heuristics and that they can be understood in physico-chemical terms; and, third, that these relationships can be used as powerful rules for rational coiled-coil peptide and protein design.

Classical coiled-coil dimers, trimers, and tetramers

Our understanding of coiled-coil chemistry leapt forward in the early 1990s through the joint efforts of the Kim and Alber laboratories. Their work centered on the GCN4 leucine zipper, **Figure 1A**. Synthetic peptides for this ≈ 30 amino-acid, 4-heptad sequence are accessible to solid-phase peptide synthesis, amenable to biophysical characterization, and crystallizable allowing the determination of highly informative X-ray crystal structures (6, 7). As a result, the parent peptide, GCN4-p1, became a model for protein folding, assembly, and stability. The rapid turnaround of GCN4-p1 variants pushed understanding of sequence-to-structure studies.

Harbury's work is particularly noteworthy (73, 74). It shows that the nature and order of **h**-type residues of the **a** and **d** sites of heptad repeats largely determine the oligomeric state of classical coiled coils. Harbury's experiments were straightforward. He made variants of GCN4-p1 with different combinations of two of the most common hydrophobic amino acids in coiled coils—leucine (Leu, L) and its isomer isoleucine (Ile, I)—at all of the **a** and **d** sites. Let us call these peptides pIL, pII, and pLL, where the first named amino acid is at **a** and the second is at **d** (**pad**). Harbury characterized the peptides in solution and by X-ray crystallography. Unsurprisingly, all were stable α -helical oligomers in aqueous buffer. The surprise was that they formed different oligomers; pIL, pII, pLI were dimeric, trimeric, and tetrameric, respectively. This was surprising because most bioinformatic analyses would consider Leu and Ile to have similar impacts on protein structure. Harbury's X-ray crystal structures explained this conundrum as described below and illustrated in **Figure 3, C–E**.

As noted by O'Shea for the GCN4-p1 dimer (6), the KIH packing at the **a** and **d** sites are different, **Figure 3C**. The $\text{Ca}-\text{C}\beta$ bond vector of Leu (the knob) at **d** points directly towards the neighboring helix and into a hole formed by side chains (at **a**, **d**, **e**, and **a₊**) of that helix (see **Fig. 2, B** and **C**). We call this packing *perpendicular*, and, overwhelmingly, it best accommodates Leu residues (37, 75). By contrast, the side chains at **a** point out of the core and towards solvent. Here, the $\text{Ca}-\text{C}\beta$ bond vector of the Ile at **a** is *parallel* to its hole on the neighboring helix, which is formed by **d₊**, **g₊**, **a**, and **d** residues. Thus, the **a** sites of dimers can accommodate many more residue types than **d**, including the bulkier β -branched Ile (37, 75).

Imagine bringing a third amphipathic helix into a dimeric assembly. Driven by the hydrophobic effect, the two original helices will respond and redirect their hydrophobic **a+d** faces

towards that of the incoming helix; effectively, these helices rotate on their own axes. As a result, the KIH packing of all of the **a** and **d** side chains will change. This is manifested in the structure of pII, which is trimeric in solution and the crystal state, **Figure 3D** (73). From this structure, the change in side-chain packing angles is clear. They are no longer perpendicular or parallel, and they are similar to each other. We call this *acute* packing. This similarity means that the amino-acid preferences at the two sites are similar (75–77). Hence, making **a = d = Ile** drives towards similar packing at the two sites and, therefore, towards trimers.

Adding a fourth helix to the assembly alters the core-packing angles (CPAs) again, **Figure 3E**. In this case, the **a** side chains pack perpendicular and those at **d** parallel. This is the reverse of the dimer. Hence, when the residues at **a** and **d** are swapped, pIL \rightarrow pLI, the new peptide forms a tetramer.

Harbury's GCN4-p1 variants have repeated cores, whereas natural sequences are more complex and heterogeneous, which bioinformatics bears out (75–77). Nevertheless, since their discovery, Harbury's basic sequence-to-structure relationships have been confirmed by analyses of many natural coiled-coil sequences and structures (37, 50, 75) and through quantitative biophysical studies (78, 79). Moreover, they have been used widely as *rules for protein design* by many groups to deliver many *de novo*-designed coiled-coil peptides and proteins (12, 14, 51, 70, 80), which are described in more detail below. A penultimate point on sequence-to-structure relationships that has emerged over the past 2 to 3 decades is that the hydrophobic cores of coiled coils tend to be built from aliphatic amino acids (A, I, L, M, and V) rather than the larger aromatic amino acids (F, W, and Y) (37, 50, 75–77). This is probably because of the limited volumes of the interhelical space and packing requirements of KIH interactions in coiled coils. Indeed, although aromatic residues can be introduced into both natural and *de novo* coiled-coil peptides, they tend to result in unusual structures that go beyond the classical and symmetric dimers, trimers, and tetramers (81–84).

That said, it is not all about aliphatic hydrophobic residues either. Approximately, 20% of the residues at the core **a** and **d** sites of coiled-coil sequences are polar, including charged residues (75–77). These reduce the thermal stabilities of the coiled-coil assemblies. However, given the hyperthermal stability possible with even relatively short coiled coils (33, 34, 85), the disruption of perfect hydrophobic repeats is almost certainly essential for protein dynamics and turnover in natural coiled coils. Moreover, these polar inclusions play important roles in specifying the correct structural state. A prime example of this is the conservation of an Asn residue at a central **a** site in the wider family of leucine-zipper transcription factors (86). The reason for this is apparent in the X-ray crystal structure of GCN4-p1 dimer, where the Asn pair can make a side-chain hydrogen bond, **Figure 3F** (6). Presumably, this offsets the energy penalty for including polar Asn in the hydrophobic core. However, as shown by reasoning, analysis, modeling, and experiments (86–88), this interaction cannot be made in alternate states such as antiparallel dimers and parallel trimers. In other words, Asn@**a** is tolerated in parallel dimers but more destabilizing in other states

and, thus, specifies the former. In protein design, this is called *negative design*, which refers to features that destabilize alternative accessible states more than the targeted state. As a result, Asn@*a* and other polar inclusions are now widely implemented in peptide and protein design and engineering (89–94). This has been formalized by Boyken and Baker in the HBNet protocol in Rosetta, which can introduce hydrogen-bond networks into coiled-coil-like *de novo* proteins beyond the canonical Asn-Asn pairs of dimeric interfaces (95) (https://www.rosettacommons.org/docs/latest/scripting_documentation/RosettaScripts/Movers/movers_pages/HBNetMover).

Beyond classical 2 to 4 helix coiled coils

The previous section shows how different combinations of mostly aliphatic residues at the *a* and *d* sites of canonical heptad repeats leads to the different parallel oligomer states: dimer, trimer, and tetramer. Examination of the high-resolution structures of the two series of peptide assemblies—namely, Harbury's engineered GCN4-p1 peptides and a set of *de novo* design peptides (73, 74, 89)—reveals that something more is going on. In short, as the oligomer state increases, more of each component helix becomes engaged in the helix-helix interfaces. This results in residues flanking the *a* + *d* seams—the *e* and *g* sites—becoming increasingly buried. Thus, potentially, KIH interactions can extend past the *a* and *d* sites in trimers and above. The idea that residues at *e* and *g* sites progressively become involved in coiled-coil interfaces with increasing oligomeric state was first formalized by Walshaw (96, 97), though Dunker and Zaleske considered the more general problem earlier (98), as did DeGrado et al. (99) at about the same time as Walshaw.

Walshaw's logic and the resulting nomenclature are straightforward: he called the *a* and *d* sites of classical coiled coils with traditional **hphhphh** repeats, "Type N interfaces". He reasoned that adding *h*-type residues—or generally, residues that can act as knobs—different coiled-coil repeats, and assemblies can be envisaged. For instance, expanding the interface with one residue gives **hphhhpp** or **hphphph** repeats, which Walshaw called Type I interfaces. The latter, with the additional knob residue at *g*, is the more likely and more common of these two repeats. Placing *h*-type residues at both *e* and *g* gives **hphhphh** repeats and Type II interfaces. As expanded below, it is helpful to consider this as two superimposed 3,4 hydrophobic repeats, **hbcdfhfg** and **abchefh** with two distinct interfaces, *a* + *e* and *d* + *g*.

For the Type I and II interfaces, the original *a* + *d* interface is simply expanded and the hydrophobic seam on one face of the amphipathic helix is broadened. As a result, more helices can be recruited to the bundle. Mistakenly, Walshaw and I thought that this would stop at six helices (hexamers) (96), but our own experiments later proved us wrong (34, 100). Finally, these expanded interfaces need not be contiguous. Repeats of the type **hhphhph** give two distinct hydrophobic seams formed by the *a* and *d* sites and the *b* and *f* sites and, thus, on the opposite sides of the helix. The resulting helices are no longer simple amphiphiles, they are bifaceted with the potential to

form high-order structures (97, 99, 101, 102). Walshaw called these Type III interfaces, which are manifested in large helical barrels such as the 12-helix assembly of TolC (103) and more recent structures of the F₁F₀ ATP synthase (104); and they are being used in design by Conticello et al. to design fibrous and nanotubular assemblies (105–107). Conticello et al. have written a comprehensive review on such structures (108).

In summary and as a rough guide: coiled-coil dimers tend to have canonical repeats and Type N interfaces; trimers have Type I interfaces; tetramers can have Type I or II interfaces and, as a result, are at an interesting tipping point between trimers and higher-order structures (100, 109); Type II interfaces tend to form pentamers, hexamers, and heptamers, but octamers and nonamers have been observed in X-ray crystal structures (40); and larger assemblies of 10 helices and above usually require Type III, bifaceted interfaces.

Testing and expanding chemical understanding through *de novo* coiled-coil design

After Feynman's epitaph, "*What I cannot create, I do not understand.*", one test of our understanding of protein structure is to build entirely new proteins from scratch. While *de novo* protein design has been active for ≈40 years, the field is now advancing rapidly and booming (51, 70, 110–112). As a result of the above understanding of their physics and chemistry, coiled coils have been favored targets for protein designers from the start (12, 14). This has led to many *de novo* coiled-coil peptides and proteins that have been characterized in solution and resolved to atomic resolution by X-ray crystallography. The history and achievements of this subfield are well documented (12, 14, 51, 70, 80), so I will not repeat it here. Instead, to illustrate the journey and progress here, rather shamelessly, I will mainly describe the rational and computational design approaches that my group has taken to deliver a set of autonomous coiled-coil peptide modules. We call this the coiled-coil basis set, which is illustrated in Figure 4.

Our original aims for the basis-set project were as follows: (1) To test and develop sequence-to-structure relationships for coiled coils in a totally synthetic and controllable framework. This was motivated by much of the work to that point being done on the GCN4-p1 system, which increasingly revealed contexts and alternate states that thwarted systematic studies (73, 75, 113). And (2), to deliver a toolkit of modules for which the role of every amino acid in each peptide was understood. In turn, this would allow the modules to be used reliably in synthetic biology to construct more complex and functional protein-like objects (114, 115).

Mimicking natural dimers, trimers, and tetramers

Our initial design approach was rational. It used 28-residue synthetic peptides, as these are accessible by solid-phase peptide synthesis and usually form stable helical assemblies amenable to full biophysical and structural characterization. The peptides had four heptad repeats with **(abcdef)₄** registers to maximize potential **gi-1 → ei** salt bridges in parallel homomers. Specifically, the repeat sequences were **(EaAAdKX)₄**,

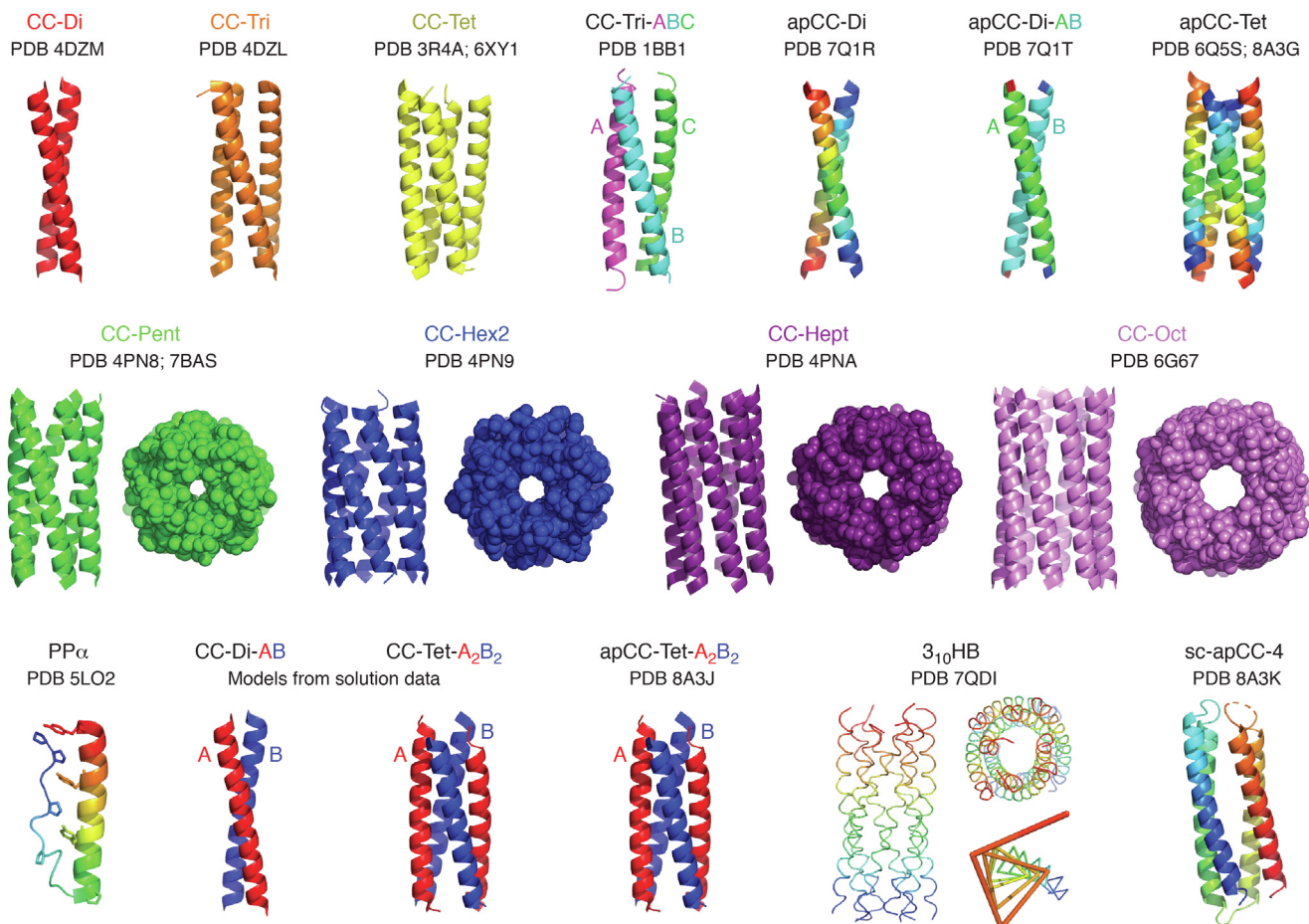


Figure 4. A gallery of *de novo* coiled-coil structures. Top row: coiled-coil bundles with two to four helices (89). Middle row: coiled-coil α -helical barrels with five to eight helices and central, solvent-accessible lumens (34, 144). The diameters of the lumens scale approximately with the number of helices in the assembly, ranging from ≈ 5 to 10 \AA . Bottom row from left to right: a monomeric single-chain miniprotein with a proline-II helix followed packing with an α helix (290); three hetero-oligomeric coiled coils formed from acidic (A, red) and basic (B, blue) peptide chains (92, 119); an 8-helix bundle formed exclusively from 3_{10} helices (52); and a single-chain 4-helix coiled coil based on apCC-Tet* (148). Key: systematic names are given above each structure, and 4-digit, PDB codes are given below; CC stands for coiled coil, and Di, Tri, Tet, etc refer to dimer, trimer, tetramer etc; all of the assemblies with helices shown in solid colors are parallel bundles or barrels; those with antiparallel arrangements of helices are colored as chainbows from the N terminus (blue) to the C terminus (red), except for apCC-Di-AB, which only has the termini colored blue and red; the systematic names for the antiparallel structures are prefixed with 'ap'. All images were made in PyMol (pymol.org) using the PDB codes given or from models generated in CCBUILDER/ISAMBARD (29, 35, 36). PDB, Protein Data Bank.

with X usually Gln, Lys, Tyr, or Trp to aid helicity and solubility and to introduce chromophores. First, we used the aforementioned combinations of Leu, Ile, and Asn at α and δ sites (73, 75) to target parallel dimeric, trimeric, and tetrameric coiled-coil assemblies. The resulting peptides were all confirmed as thermostable, cooperatively folded, helical oligomers in solution by CD spectroscopy, and with the intended oligomeric states using analytical ultracentrifugation (89). Moreover, high-resolution X-ray crystal structures revealed the targeted parallel dimer, trimer, and tetramer, CC-Di, CC-Tri, and CC-Tet, respectively, Figure 4, (89, 100).

Next, starting from CC-Di, we designed obligate heterodimers. This adopted straightforward design principles from O’Shea & Kim (116) and Hodges (117, 118) in which complementary acidic (A) and basic (B) chains are achieved by making $g = e = \text{Glu}$ and $g = e = \text{Lys}$, respectively. This delivered CC-Di-AB variants with fully quantified affinities in the μM to sub-nM range (92). This principle has also been applied to give an A_2B_2 tetramer, CC-Tet-A₂B₂, Figure 4 (119). Previously,

with Alber, we had used the idea of electrostatic heterospecification in computational design to make a heterotrimer, CC-Tri-ABC (120), a structure for which was later determined by X-ray crystallography, Figure 4 (121). This target has been revisited by Baker et al. using parametric design in Rosetta (122).

Many others have developed heterodimeric AB systems, including the following: the aforementioned designs from O’Shea and Kim, “peptide Velcro” (116), and from Litowski and Hodges, “E/K coil” peptides (117, 118); Keating’s “SYN-ZIP” designs (123, 124); and the sets of coiled-coil heterodimers from Jerala (91, 125) and Mason (93). Interestingly, as we have also found, it appears difficult to obtain crystals and solve structures for heteromeric *de novo* coiled coils, and few have been resolved to high resolution (126). Nonetheless, these systems are being put to good use in a variety of applications, including the following: driving membrane fusion (127, 128); directing the patterned aggregation of bacterial and human cells (129); developing peptide origami by Jerala (65, 80, 130);

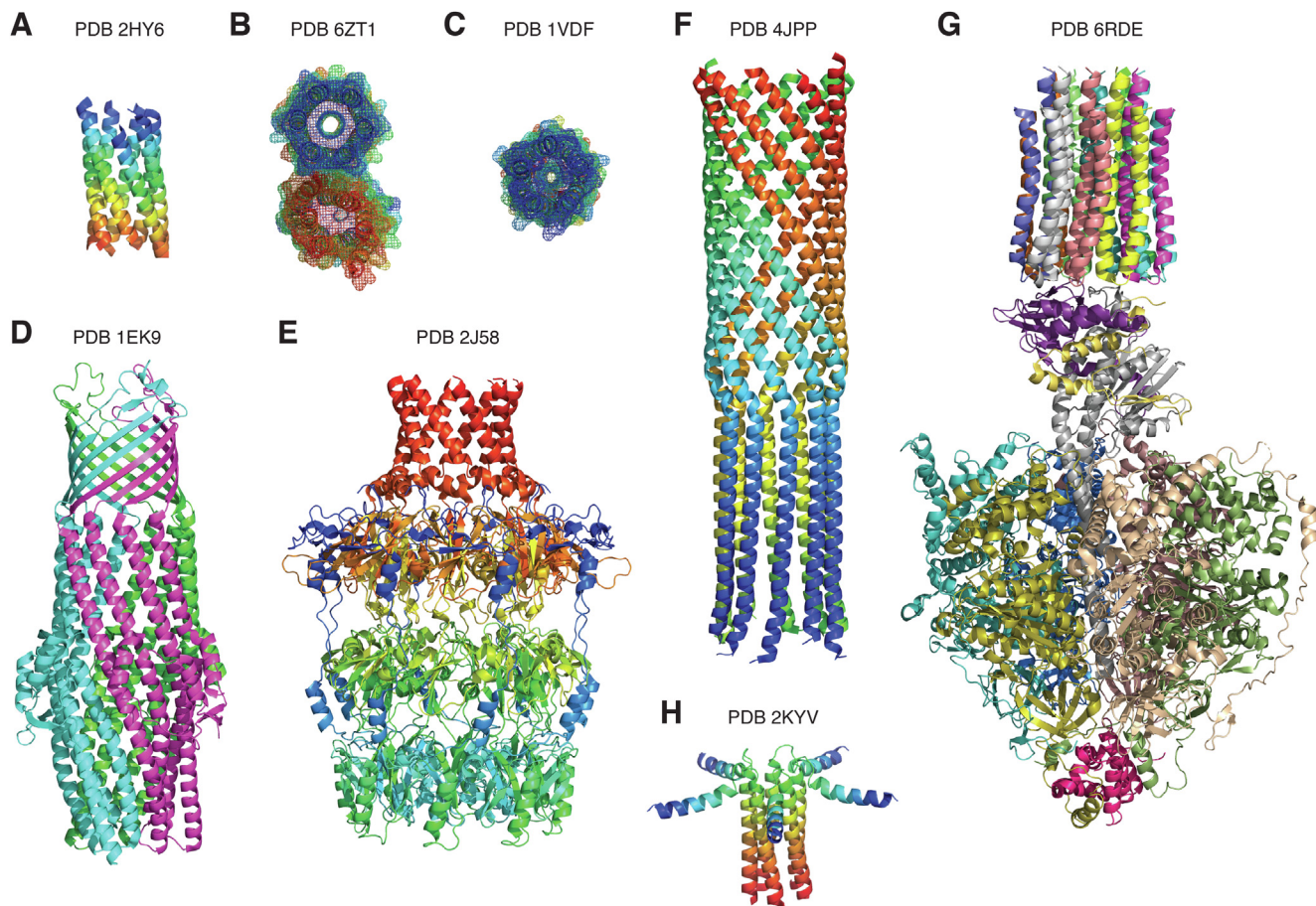


Figure 5. Structures of designed and natural α -helical barrels. *A*, a slipped heptamer formed by a mutant of GCN4-p1 peptide with Ala at the **e** and **g** positions (2hy6 (138)). *B*, a designed hexameric coiled coil with Gly at the **e** sites that accesses both closed and open states in the crystal and solution states (6zt1 (145)). *C*, the natural pentameric coiled coil of cartilage oligomeric matrix protein, COMP (1vdf (243)). *D*, the trimeric TolC protein from *Escherichia coli* (1ek9 (103)). This spans the periplasmic space to link the inner and outer membranes to allow efficient efflux from the cell. The upper β -barrel spans the outer membrane, the central 12-helix α -barrel bridges the periplasm, and the lower antiparallel coiled-coil dimers engage other proteins of the efflux machinery at the inner membrane. *E*, the octameric Wza protein from *E. coli* (2j58 (244)). This exports polysaccharides for assembly on the outer surface of the bacterium, with the upper part forming an 8-helix barrel in the outer membrane. *F*, the H protein from the $\Phi X 174$ coliphage forms a 10-stranded α -helical tube, which can span the periplasm of the host to deliver its ssDNA genome (4jpp (291)). Note how the coiled coil switches from right-handed (near straight) at the *N* terminus (*bottom*) to left-handed at the *C* terminus (*top*). *G*, cryo-EM structure of the $F_1 F_0$ ATP synthase from a green alga (6rde (104)). The membrane-spanning *c*-ring, which comprises concentric rings of coiled-coil helices (*top* of the cartoon), couples proton transport to rotatory catalysis in the F_1 assembly (*bottom*) via a central stalk, the γ subunit, which is an antiparallel coiled-coil dimer (slightly obscured and colored silver). *H*, a pentameric NMR ‘pinwheel’ structure for cardiac-muscle phospholamban (2kyv (272)). Although SOCKET analysis reveals a clear pentameric α -helical barrel, the central pore is too narrow to act as an ion channel. This structure is proposed to be the dominant T state in the membranes. Chain coloring varies between the panels: in *A*, *B*, *C*, *E*, *F*, and *H*, chainbows are used to trace the *N* to *C* termini of the different chains; in *D* and *G*, the protomers are each colored differently. In panels *B* and *C*, the atomic surfaces are shown meshed.

as “peptide-PAINT” or “live-PAINT” for high-resolution light microscopy (131, 132); and targeting natural coiled coils *in vitro* and in cells (133–137).

Exploring the dark matter of coiled-coil space – α -helical barrels

The basis-set peptides led to two serendipitous discoveries. First and surprisingly, a permutation of CC-Tet with the repeat changed from EIAALKX to EIKALAX—which moved an Ala to **e**—formed a parallel hexamer, which we named CC-Hex (100), Figure 4. This resonated with Lu’s discovery that a permuted of GCN4-p1 with **e** = **g** = Ala gave a slipped heptamer (138), Figure 5A. Thus, as introduced above, expanding the **a+d** hydrophobic seam to include small hydrophobic residues at **g** and **e** recruits more helices to coiled-coil assemblies.

These discoveries are interesting for two reasons: (1) The vast majority of natural coiled coils are dimers, trimers, or tetramers (19, 20, 50, 67). Thus, the hexamer and heptamer open up potential “dark-matter” protein structures to explore and exploit (139, 140). And (2), both have central and fully accessible channels, Figures 4 and 5, making them α -helical barrels (α HBS) rather than α -helical bundles with consolidated hydrophobic cores. As described below, this opens possibilities for functionalizing *de novo* coiled-coil scaffolds considerably. However, to realize this, CC-Hex and other α HBS would have to be robust to mutation. Despite some early successes (141), we found that CC-Hex often collapsed back to parallel tetramer and other states when altered. Therefore, to deliver other and more robust α HBS, we turned to computational protein design. This required the development of in-house parametric coiled-coil design tools (29, 35, 36) and the

application of scoring methods from Keating (142) to assess the helix–helix interfaces. This delivered new and robust sequences for parallel and nonslipped pentameric, hexameric, and heptameric coiled coils, CC-Pent, CC-Hex2, and CC-Hept, which were all confirmed in solution and by X-ray crystal structures, Figure 4 (34).

Interestingly, the computational α HB designs have sequences related to the initial rational and serendipitous designs, namely, the **a** = Leu plus **d** = Ile core from CC-Tet and CC-Hex is preserved; as introduced above, the **e** and **g** sites are more intimately involved in the helix–helix interfaces and tend to be more hydrophobic; and, consequently, the interhelix salt-bridging Lys and Glu residues are moved to **b** and **c**, respectively. Incidentally, for the computationally designed α HBs, and for most subsequent designs of higher-order coiled coils, we have changed from sequence repeats with **g**–**f** register to **c**–**b** registers (34). This maximizes interhelical salt bridges: in classical parallel dimers and trimers, these salt bridges can form between residues at **g** on one helix and residues at **e** of the next heptad in the neighboring helix, i.e. **g**–**e**'₊₁ (89); in parallel pentamers and above, they are at **c**–**b**'₊₁ (34); and parallel tetramers fall between these extremes (143).

Finally on the chemistry of α HBs, there is a conundrum for the natural and serendipitously discovered barrel-like proteins. A basic tenet of coiled-coil assembly—and protein folding in water generally—is that the polypeptide chains fold to minimize their free energy, with a major part of this coming from burying their hydrophobic side chains to form a hydrophobic core. Thus, how do α HBs with predominantly hydrophobic residues at the lumen-facing **a** and **d** sites avoid collapse? Again, the answer lies in the stereochemistry of core packing.

Further empirical studies of the computationally designed α HB sequences have revealed the importance of β -branched residues at the **a** and **d** sites in maintaining the barrels (144): for open channels, the **d** sites must be predominantly Ile or Val in combination with **a** = Leu, Ile, or Val. Relaxing this and allowing **d** = Leu leads to collapsed high-order oligomers with consolidated cores. Furthermore, we have found that the residues at the **e** and **g** positions also have profound and different effects on α HB formation and oligomeric state. For example, in parallel α HBs, side chains at **g** point directly towards the neighboring helices—they pack perpendicularly into **e**'**a**'₊₁**b**'₊₁**e**'₊₁ holes (discussed below and illustrated in Fig. 6). As a result, the oligomeric state is very sensitive to the size of the side chain here. For the same sequence background, the series Gly → Ala → Ser → Thr at **g** form nonamer, heptamer, hexamer, and pentamer, respectively (40), Figure 4 and Table 1. That is, smaller side chains allow closer helix–helix contacts and, thus, recruitment of more helices to the barrel. By contrast, similar changes at **e** have less predictable effects, leading to α HBs, collapsed structures, and other helical bundles (Martin *et al.*, unpublished data). Intriguingly, a sequence with Gly at **e** forms both open-barrel and collapse hexamers in the same crystal structure (Fig. 5B) and in solution (145). It appears that the introduction of Gly@**e** relaxes the helix–helix interactions sufficiently to allow both close helix–helix contacts and hydrophobic collapse, but with the open α HB still energetically accessible (145).

Extending the parametric coiled-coil model

This expansion of coiled-coil structural space presents an opportunity to examine how coiled-coil geometry changes with oligomer state. To do this, Prasun Kumar compiled data for all-parallel coiled coils from the 2022 update of the CC+ database (50). As expected, the radius of the coiled-coil superhelix increases with oligomer state, Figure 6A. Turning to superhelical pitch, Figure 6A, for dimers through hexamers, these are near the theoretical value of ≈ 200 Å, although there is considerable variation around this. For heptamers and octamers, there is a sharp increase in coiled-coil pitch. Most likely, this is due to straightening of the coiled coil needed for peripheral KIH interactions by residues at **e** and **g** to be made, though there are still very few high-resolution structures for these coiled coils to make firm conclusions.

A closer examination of KIH interactions made by side chains at **a**, **d**, **e**, and **g** sites in the dataset is interesting, Figure 6B. The aforementioned systematic changes in CPAs of residues at **a** and **d** between parallel (≈ 0), acute (≈ 45), and perpendicular (≈ 90) packing (see Fig. 3, C–E) are clear for the dimers, trimers, and tetramers. Extending this beyond tetramers, a number of things become apparent: first, the CPAs at the **a** and **d** sites change little above tetramer. Indeed, they asymptote to $\approx 115^\circ$ (near perpendicular) and $\approx 25^\circ$ (near parallel), respectively. Second, KIH packing at the **e** and **g** positions only come into play for tetramers and above: for tetramers and pentamers, KIH interactions are made here $\approx 50\%$ and $\approx 75\%$ of the time, respectively; for the hexamers, $>90\%$ of side chains at these sites make KIH interactions; and for the few examples of heptamers and octamers, all residues at both **e** and **g** positions act as knobs, i.e., they are fully Type II interfaces. This is why the tetramer is a tipping point between classical (Type N and Type I) and higher-order (Type II) coiled coils. Third, when KIH interactions are made by residues at **e** in tetramers and above, the CPA is $\approx 30^\circ$ regardless of oligomer state and the packing is like that at **d**, whereas, at **g**, the CPA changes from $\approx 95^\circ$ for tetramers to $\approx 60^\circ$ for the octamers. Thus, in the higher oligomers, side chains at **e** make parallel KIH interactions and those at **g** perpendicular interactions. This is why side chains at **g** have a greater influence on coiled-coil structure and stability than those at **e**, as noted above (Table 1 and reference (40)).

Finally, a simple model using projections on idealized, 3.5-residues per turn helical wheels captures many of the changes in CPAs and KIHs, Figure 6, C and D. This is my zeroth-order attempt to include side-chain packing geometries in Crick's coiled-coil parameterization. It will be developed elsewhere as it may be of use to others engaged in rationalizing complex, natural coiled-coil structures or designing them rationally and computationally.

Targeting antiparallel structures

Our second serendipitous finding was that certain CC-Hex variants formed another coiled-coil state, an antiparallel tetramer (109). The *de novo* design of 4-helix bundles with antiparallel, up-down-up-down topologies is a large field in itself. As reviewed elsewhere (70, 146, 147), these have been design targets for DeGrado, Dutton, their former group

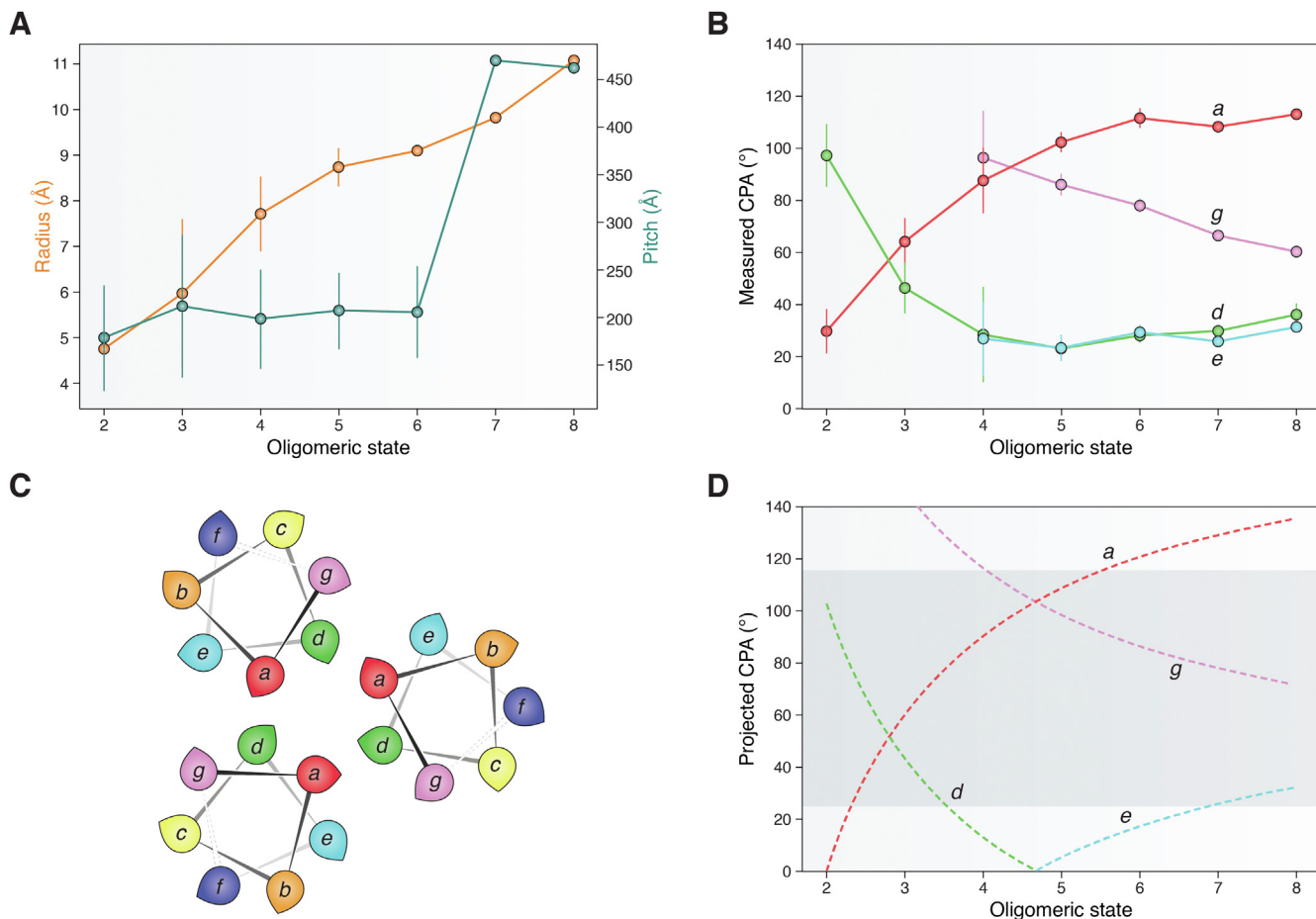


Figure 6. Structural parameters and knobs-into-holes packing and core-packing angles in more detail. A, how coiled-coil radius and superhelical pitch change with oligomeric state for 175 all-parallel structures from the 2022 version of the CC+ database (50). **Search parameters:** SOCKET packing cutoff, 7 Å; sequence redundancy, 50%; helix orientation, all parallel; number of helices, 2 to 8; experimental method, X-ray crystal structures at 2.2 Å resolution or better. B, how the CPAs calculated by SOCKET (37, 39) made by side chains at the **a**, **d**, **e**, and **g** sites in the same dataset change with oligomeric state (10,164 CPAs in total). The error bars are for 1 SD; and the points are joined by lines simply to guide the eye. C, a simple geometric model for CPAs based on an idealized, flat, helical wheel (*i.e.*, with 3.5-residues per turn) for the heptad repeat. In this model, CPAs are approximated as the angles made between vectors for the knob residues (**a**, **d**, **e**, or **g**) and the bases of the holes. The knob vectors are taken as extensions of the preceding Ca-Ca virtual bond vectors as indicated by the directions of the colored teardrops. The base vectors are corresponding Ca-Ca virtual bond vectors as follows: CPA_a = **ga** into **ga**; CPA_d = **cd** into **de**; CPA_e = **de** into **dc**; and CPA_g = **fg** into **ab**. When considered for different oligomer states, this results in the following equations: CPA_a = 180° - 360/N; CPA_d = 360/N - 77; CPA_e = 77 - 180/N; and CPA_g = 360/N + 26; where N = oligomeric state. D, plot showing how these projected CPA values vary with oligomer. The zone where most of the experimentally observed CPAs (calculated by SOCKET) occur is shaded gray. The color schemes of panels B and D are matched. CPA, core-packing angle.

Table 1

Design rules for coiled-coil oligomers

name Oligomer	<i>a</i>	<i>b</i>	<i>c</i>	<i>d</i>	<i>e</i>	<i>f</i>	<i>g</i>	PDB code
CC-Di	I/N	A/X	A/X	L	K/E	X	E/K	4dzm
CC-Tri	I	A/X	A/X	I	K/E	X	E/K	4dzl
CC-Tet*	L	K/E	E/K	I	Q	X	Q	6xy1
CC-Pent*	L	K/E	E/K	I	A	X	T	7bav
CC-Hex2	L	K/E	E/K	I	A	X	S	4pn9
CC-Hept	L	K/E	E/K	I	A	X	A	4pna
CC-Oct	I	K/E	E/K	I	A	X	A	6g67
CC-Non	L	K/E	E/K	I	A	X	G	7bim
apCC-Tet*	L	EEKK	EEKK	I	A	X	Q	8a3g

Left-hand column, systematic name of the *de novo* coiled-coil assembly (Fig. 4). **Right-hand column:** PDB code of a representative structure for the design. **Middle columns:** favored amino acids at the seven sites of the coiled-coil heptad repeats, **abcdefg** for the coiled-coil state. **Important note on register:** Straight **a** – **g** registers are usually not used in *de novo* coiled coils. Rather, in parallel dimers and trimers, the sequence repeats are **g** → **f**. This is because side chains at **g**₋₁ of one helix can make interactions with those at **e** of the following heptad repeat on a neighboring helix; for example, to make **g**₋₁ → **e** salt bridges. However, for parallel tetramers and above, because side chains at **e** and **g** become increasingly involved in helix–helix interactions, the salt-bridge interactions are moved to **c** → **b**₊₁. Hence, the sequence repeats of these higher-order oligomers are best constructed with **c** → **b** register repeats. **Key:** standard one-letter codes are used for the amino acids; X = any proteinogenic amino acid except Pro. **Note:** as discussed in the text, although the sequence-to-structure relationships summarized here have been determined bioinformatically, computationally, or empirically and tested in multiple experiments, they are not all hard-and-fast rules. Also, they have largely been developed and tested in the context of 4-heptad sequences. Thus, they may be subject to context dependence.

members, and more recently by computational designers. Nevertheless, we were interested in exploring this region of coiled-coil sequence and structure space both to avoid unwanted alternative states in α HB design and to define rules for a new basis-set member; *i.e.*, apCC-Tet, where the ‘ap’ prefix signifies antiparallel.

The initial antiparallel-tetramer variants of CC-Hex were far from ideal (109). Through a series of rational redesigns, we arrived at a sequence of apCC-Tet for which the solution-phase and X-ray crystal data concurred (109), Figure 4. Subsequently, we have conducted a systematic rational and computational design of new apCC-Tet variants, leading to more robust sequences and structures for both homo and heterotypic antiparallel coiled-coil tetramers. Moreover, these helical sequences can be linked with turns and loops to render a single-chain anti-parallel 4-helix coiled coils, sc-apCC-4, in a single design step (148). This whole process has been followed at atomic resolution with X-ray crystal structures for apCC-Tet*, apCC-Tet-A₂B₂*, and sc-apCC-4, Figure 4. Thus, we have graduated from peptide to protein design using robust and rational design rules. This followed the pioneering work of Regan and DeGrado and by Hecht and the Richardsons (149, 150). From our recent studies (148), the following rules and principles emerge for antiparallel coiled-coil tetramers: the use of **a** = **d** = Leu or better **a** = Leu **d** = Ile cores; an obligate Ala at **e**, similar to so-called Alacoils (151); a preference for Gln at **g**; and the use of charge complementarity at **b** & **c** as a final guide to helix-helix specification and orientation, and specifically, using oppositely charged residues in the *N*- and *C*-terminal halves of these designs (152–154).

The design of antiparallel coiled-coil dimers has been pursued by others for some time; for examples, see the work of Hodges, Oakley, Gellman, Keating, and others (152–159). However, only one of these has been confirmed by a high-resolution X-ray crystal structure (160). Therefore, we were keen to add apCC-Di sequences and structures to the basis set. A challenge here is that, while antiparallel 2-helix coiled coils dominate coiled-coil structures in the PDB (37, 50), these are mostly intramolecular helix-turn-helix structures. Thus, some of the structural *specification* is from the proximity of the two helices in the sequence. As a result, true and robust sequence-to-structure relationships are difficult to decipher (37, 161). Nonetheless, recently with the Hoecker group, we have designed homomeric and heteromeric antiparallel dimers (162), Figure 4. We achieved these by combining bioinformatic analysis to discover new design rules and empirical rational design. Interestingly, we find that the basic peptide of the antiparallel heterodimer, apCC-Di-B, is a highly efficient cell-penetrating peptide, which, once inside mammalian cells, localizes to proteins of interest fused to its partner apCC-Di-A (162).

Current rules and challenges in coiled-coil design

Our current set of sequence-to-structure relationships or rules for the coiled-coil design and the basis set are summarized in Table 1. These are constantly being modified, improved, and expanded upon (40, 109, 143, 148, 162), and iterations will likely be necessary to hone designs for

applications in chemical and synthetic biology. Indeed, our current design rules and structures are based on repetitive, heptad-centric, and low-complexity sequences. By contrast, natural and some of the computationally designed coiled-coil sequences show more variability. As discussed later, this leaves room for understanding natural coiled coils better and interesting prospects for developing and exploiting new coiled-coil designs. Aligned to this, the original CC-Hex offers a cautionary tale (100): it is clear that this state—the parallel hexamer—is close in energy to the parallel and antiparallel tetramer states (100, 109). While this creates a productive playground for coiled-coil discovery, it also highlights a complex free-energy landscape with multiple states close in energy that must be navigated carefully (109, 144, 145). Exploring other sequence repeats and mixing and matching those available to increase sequence complexity may help address this issue; indeed, others like Mason, Keating, and Jerala are showing the way here (93, 124, 163).

Putting *de novo* coiled coils to use

It is one thing to deliver toolkits of *de novo* peptides and proteins, it is another to do something useful with them. Here, I outline potential uses of our and other coiled-coil modules.

Functional designs that we have demonstrated using CC-Di and CC-Di-AB, apCC-Di and apCC-Di-AB, CC-Tri, CC-Tet, and related peptides include the following: the construction and application of Self-Assembled peptide Fibers, SAFs (164), and hydrogel-forming variants of these, hSAFs (165); the templated assembly of bacterial collagens (166); the design of Self-Assembled peptide caGEs, SAGEs (167) and the applications of these in cell delivery and vaccine development (168, 169); the construction of artificial transcription factors (119, 170) and cytoscaffolds (171) that assemble and function in bacterial cells; the directed assembly of large DNA origamis (172); the presentation of functioning hotspot residues from natural protein–protein interactions (173); the direction of protein–protein interactions at synthetic (174) and biological (175) membranes and controlling the former by incorporating phosphorylation-based switches into the designs (174); and, most recently, cell penetration and subcellular targeting in mammalian cells (162).

Our adaptations of the α HBS have included the following: assembling peptide-based fibers and nanotubes (176, 177), following the approach of Conticello (178); installing a Cys-His-Glu catalytic triad in the channel of CC-Hept to effect ester hydrolysis; developing receptors for reporters dyes and lipophilic biomarkers that bind within the channels with μ M affinities (179) and using this as the basis for a differential biosensor (180); redesigning water-soluble α HBS to produce a membrane-spanning ion channel with high conductance and selectivity (181); and designing a system that switches between the open- α HBS and collapsed states, Figure 5B (145).

Perhaps, the most used *de novo* coiled-coil modules have been CC-Di-AB (92) and related heterodimeric systems, such as Hodges’ E/K peptides (117, 118), Keating’s SYNPZIP systems (124), and others from Jerala (91, 94), Mason (93, 182), O’Shea

(116), and Vinson (183). This plurality of heterodimeric modules has helped advance synthetic biology, vesicle/protocell work, and protein origami, as reviewed elsewhere (15, 16). This widespread use is almost certainly because of a trinity of simplicity, robustness, and utility of these systems. They are *simple* as they comprise two short (\approx 30-residue) polypeptides, usually with one basic and one acidic. They are *robust*, as invariably, they form obligate, stable heterodimers as designed. And they have *utility* because (i) they are readily made by solid-phase peptide synthesis or as fusions to proteins of interest *via* gene synthesis and recombinant expression; (ii) they can be adapted to render a range of association constants from μM to pM (92, 183); and (iii) in several cases, multiple orthogonal pairs have been engineered (91–94, 124, 182).

Applications by others of CC-Di-AB include the following: designing self-sorting heterodimers (184); developing a fluorescence-quencher pair that reports on coiled-coil stability and orientation (185) and, similarly, coassembled fluorescent proteins (186); constructing synthetic virus-like capsids (187) and motor proteins (188); examining models for strand displacement in peptide-peptide interactions (189); exploring the mechanics of biomaterials using biomolecular simulations and experiments (190–192); engineering hybrid (natural plus designed) artificial transcription factors in *Escherichia coli* (193); designing molecular switches (beacons) for detecting natural proteins (194); masking therapeutic antibodies that can be activated by proteolysis of the coiled coils (195); and appending them to natural bacterial proteins to direct fiber formation (196).

Turning to the original basis set of CC-Di, CC-Tri, and CC-Tet, others have used these to make standards for protein oligomers, for instance GFP fusions (197, 198), though there are cautionary tales here too (see below); to construct artificial cages by appending CC-Tri, CC-Tet, or CC-Pent to natural proteins with complementary symmetries (199–202); to form defined oligomers of photosynthetic reaction centers in membranes (203); to display multiple sugar moieties (204), small-molecule-binding peptides (205), membrane-active peptides (175), and functional proteins (206, 207) on oligomeric protein scaffolds; in combination with metal coordination, to drive supramolecular assembly (208, 209); to design metalloproteins (210); and to explore the fundamentals of coiled-coil assembly (211), including the incorporation of nonproteinogenic amino acids (212).

Extending this to the oligomers above tetramer and the α HBS, others have employed these to engineer antiparallel hexamers with aromatic cores that might be suitable for electron transfer (82, 83); to direct the assembly of reversible protein condensates in living cells (213, 214); to encapsulate carbon nanotubes with these water-soluble peptides (215); to explore valency effects in natural protein-protein interactions, *e.g.*, galectin-glycan binding (216); to develop Spy&Go, augmenting the widely used SpyCatcher system through multimerization (217); and to facilitate the engineering and *de novo* design of transmembrane proteins (218, 219). Specifically on the latter, the DeGrado and Baker groups have used sequence-to-structure relationships garnered from the α HBSs to stabilize

pentameric bundles of phospholamban (218) and in the *de novo* design of ion channels (219), respectively. Finally, in an impressive series of studies, Champion et al. have shown that the original CC-Hex sequence can be complexed with IgG to promote the cellular uptake and cytosolic delivery of these antibodies (220–223).

A note of caution

Despite the sequence-to-structure relationships developed, the array of modules delivered, and the many atomic-resolution structures determined, it is important to remember that all of the *de novo* coiled coils described above are short peptides with low-to-medium sequence complexity. As a result, a number of coiled-coil assemblies are likely to be close in free energy, and multiple states could be accessible for a given set of conditions. Thus, when adapting and applying these coiled-coil modules, perturbations to the system may well shift the free-energy landscape leading to structural switching and promiscuity of interactions. Indeed, we have observed this for CC-Tet and some α HB systems (89, 100, 109, 144, 145, 181), and others have reported changes in oligomer states when incorporating some of the modules into larger fusion proteins (197, 198). Thus, some care should be taken when “plugging and playing” *de novo* and even natural coiled-coil peptides, particularly when designing linkers to them and adapting or truncating them from the 4-heptad parents. In short, the final constructs should be tested for the preservation and integrity of the intended oligomeric and orientation of the coiled-coil interactions.

The biology of coiled coils: Old frontiers comes back into view

Why I have left this section until last

It might seem odd that I am closing this perspective with the biology of coiled coils rather than starting with it. After all, much of the motivation for examining biological macromolecules comes from the fascination of what they do in biology. However, I have kept this subject to last for three reasons.

First, the vast majority of coiled-coil research has focused on the chemistry and physics of coiled coils, *i.e.*, on their sequences and structures (20, 21). Much of the early work was on two general classes of coiled coils: long fibrous coiled coils in motor proteins and intermediate filaments (IFs), which were among the first targets in structural molecular biology (21, 224); and short oligomerization domains like the leucine zippers (5), which became a model for protein folding, structure, and design (6, 7, 73). Possibly as a result of this, many biochemists and cell biologists regarded coiled coils as simple oligomerization domains and molecular spacers, with the *interesting stuff* going on elsewhere in the proteins. However, even the apparent simplicity of the leucine zippers belies an underlying complexity, which includes many proteins in humans, the specification of homo- and hetero-oligomers between these, and differing levels of expression, which combine to give exquisite control over transcription (137, 142, 225, 226).

Second, as I and others argue (70), the chemistry and physics of coiled coils are largely done. True, there are still challenges. For instance, we need to complete the sequence-to-structure relationships for some remaining coiled-coil topologies that we do not understand. Also, we need to make the prediction of coiled-coil oligomer state and stability more quantitative. This will allow possible alternative coiled-coil states to be predicted and distinguished better *in silico*. These problems will be solved. Thus, now it is time to focus back on the biology: we should be doing *coiled-coil structural biology* in the context of biology and ideally *in situ* rather than in computers or test-tubes.

Third and finally, I contend that we now have the tools to tackle coiled-coil structure and function holistically. The first of these is sequence prediction. The old view that coiled coils are simply oligomerization domains and spacers changed with improved abilities to spot coiled-coil sequences in proteins using computational biology (227), see Box 2. These coupled with genome sequencing have led to coiled-coil predictions for whole genomes (228–233). There is a cautionary note here, however, coiled-coil predictions at scale can be unreliable (234). Nevertheless, coiled coils are everywhere and perform many functions. Estimates across all genomes suggest ≈0.5 to 6.5% of protein sequences contain coiled-coil regions (232). These predictions and the increased numbers of structures have led to coiled-coil databases that are wonderful resources for biological research (Box 2). The second set of tools is around modeling. The parametric modeling of coiled-coil structures is now well established, reliable, and accessible to all (Box 2). Moreover, we are now in the post-AlphaFold era of biological research (3, 4). In my view, AlphaFold2 is one of the best hypothesis generators that we have ever had, and it will have a great impact on how we do molecular cell biology, including that involving coiled coils. Indeed, this is already becoming apparent with AlphaFold2 guiding experiments and aiding structure determinations of coiled coil-containing systems, often with unexpected results (235–240).

In summary, with a good physical and chemical understanding of coiled coils, and computational tools in place for coiled-coil prediction and modeling, we are in a strong position to address key questions in coiled-coil biology. This is not an exhaustive list, but some of these include the following: understanding important biophysical properties such as coiled-coil dynamics, exchange, and turnover; moving beyond coiled coils as simple oligomerization domains and spacers and exploring the complexity of coiled-coil architectures in the context of larger and functional biological assemblies (235, 240). That is for the future, for now, I offer a snapshot of coiled-coil structure and function as I see it currently.

A brief survey of coiled-coil function

Coiled-coil function has been surveyed in good reviews over the years (8–11, 13). The most contemporary and a particularly useful review is by Hartmann (241). Therefore, here, I give a slightly different slant on coiled-coil functions. I focus on those where I see scope for advancing our understanding in the near

future. However, because of the foregoing reviews, I do not cover any category exhaustively.

A multitude of oligomerization domains

Coiled coils are one of the nature's favored protein-oligomerization domains. Although the chemistry and design sections above illustrate the potential of coiled coils to span many oligomeric states and topologies, those in natural oligomeric proteins tend to be dominated by dimers and trimers. This can be seen by searching the CC+ database (50), Table 2, which reveals a preponderance of parallel dimers and trimers and fewer parallel and antiparallel tetramers in approximately equal numbers. Beyond these, the number of higher-order coiled-coil oligomers drops off rapidly. However, the most abundant class of coiled coil is the antiparallel arrangement of two helices in the same protein chain. Nonetheless, clearly, there is an abundance of coiled-coil-based oligomerization domains for structural and cell biologists to examine and exploit. Moreover, I am sure that this will grow with the application of AlphaFold2 to entire proteomes and the development of AlphaFold2 Multimer (3, 4, 242).

Barrels and tubes

The design section introduced the concept of α HBS, that is coiled-coil assemblies with five or more helices and central, solvent-accessible channels. From that, rational and computational peptide/protein design and engineering has delivered many examples of these, Figures 4 and 5, A and B (33, 34, 40, 100, 138, 144). However, α HBSs were first observed in nature. Early examples include the following: the pentameric cartilage oligomeric matrix protein, COMP, Figure 5C (243); the 12-helix multidrug efflux protein from *E. coli*, TolC, Figure 5D (103); the polysaccharide transporter, Wza, which is also from *E. coli* and has an 8-helix, transmembrane α HB, Figure 5E (244); and, most recently, cryo-EM structures of the F₁F₀ ATP synthase complex is revealing coiled-coil interactions in the membrane-spanning c-ring, Figure 5G (104), which can have different numbers of helices depending on the organism. A particularly interesting example is the H protein from bacteriophage Φ X174, which forms a tube that is essential for the virus to infect *E. coli* and is believed to transfer the viral ssDNA across the host periplasm. The tube is a long decameric barrel with both heptad-based left-handed and hendecad-based, right-handed coiled-coil segments, Figure 5F. As discussed in

Table 2

Dominant oligomers in the CC+ database of structurally defined coiled coils

Type	Number of helices and arrangement, parallel (p) or anti-parallel (ap)							
	2		3		4		>4	
	p	ap	p	ap	p	ap	p	ap
multichain	455	356	189	114	79	126	50	10
same chain	287	2202	7	553	0	105	0	3

Search parameters: 50% sequence redundancy; taken from the new 2022 CC+ database (<http://coiledcoils.chm.bris.ac.uk/CCPlus/Statistics.html>; Kumar *et al.*, unpublished).

previous sections, α HBs have expanded our understanding and our reach into coiled-coil structural space, and they have inspired new protein designs (13, 140, 245).

From rigid rods to flexible coiled coils in motor-protein function

The eukaryotic molecular motors of the myosin and kinesin families are often cited as archetypal examples of proteins with long coiled-coil rods. By engaging with actin filaments, muscle and nonmuscle myosin-2 generate force in muscle and to alter cell shape and drive cell motility, respectively, while myosins 5 and 6 transport vesicles over short distances. On the other hand, kinesins engage microtubule tracks, and their key activities include long-distance intracellular transport, for example, in the neuronal axon and controlling the dynamics of the mitotic and meiotic spindles in cell division. Myosins and kinesins are both large families of proteins. However, most have a similar overall domain structure comprising a head (motor) domain that engages the track and a long coiled-coil tail. Typically, these coiled coils form parallel dimers, which allow two heads to engage with the track and facilitate processive movement along it. The coiled-coil dimers are often depicted as extended and rigid rods. However, as has been known for some time (246, 247), there is a lot more to these coiled-coil proteins than the simple text-book picture portrays. For example, in striated muscle, the coiled-coil domains assemble myosin-2 into filaments, which, along with other proteins, combine with actin filaments to form the sarcomeres that are responsible for muscle structure and function. And, among other functions, the coiled coils of the kinesin-1 heavy chains complex with those of kinesin light chains, which bring important cargo-binding and regulatory features to the kinesin complex. Rather than dwell on these structures and functions, generally, I want to highlight recent advances in understanding the autoinhibited forms of the two proteins. These states are critical for controlling the functions of the ATP-driven motor proteins and, thus, for energy conservation by cells.

To myosin-2 first, it has been known for some time that the myosin-2 dimer adopts two conformations distinguished by sedimentation: a phosphorylated 6S form is the active “extended” state, and a dephosphorylated 10S is the inhibited state. Recent near-atomic resolution, cryo-EM structures of the 10S form reveal that the coiled coil nearest the head domains folds back onto these domains to form a compact structure and contributing to the mechanism of inhibition, Figure 7A (248–250). A similar theme has emerged for the heterocomplex of the heavy and light chains of kinesin-1 (240). Again, two forms of the complex are evident in sedimentation experiments and low-resolution electron micrographs. And, again, these correspond to active extended and autoinhibited compact states. However, in kinesin-1, the coiled coil folds back on itself. This is implied by an AlphaFold2 model of the complex, which fits neatly into class averages for the compact form from cryo-negative-stain electron micrographs, Figure 7B

(240). Moreover, removal of link between two of the coiled-coil segments implicated in this folding results in a permanently extended and active mutant of the complex.

Other cytoskeletal components

Sticking with parallel dimers, the IF proteins were among the first-studied coiled coils (21). With actin filaments and microtubules—which are assemblies of globular proteins—IFs are one of the three principal fibrous components of the eukaryotic cytoskeleton. There are many IF proteins (\approx 70 genes in humans) and many isoforms of these. They have been classified into six different types that are expressed and coexpressed differentially in different cells. Their precise and different roles remain poorly understood and ripe for combined structural-, cell-, and synthetic-biology research. What is clear is that IFs have central, segmented, coiled-coil rods that are responsible for dimer formation and subsequent tetramerization. In addition, terminal domains, which appear to be largely unstructured in isolation, contribute to IF assembly and function. Despite considerable effort, there is no complete atomic structure for any IF protein, not even for the coiled-coil rod, although, of course, it is now possible to generate AlphaFold2 models, Figure 7C. Instead, Strelkov et al. have applied a divide-and-conquer plus modeling approach to build a structural picture of this abundant and complex class of molecules (224, 251). Despite the apparent rigidity and stability of these IF coiled-coil assemblies, regions of the structure have been shown to be more labile, which may impact on folding, assembly, function, and malfunction (252, 253).

Dynamics at the extreme: Coiled coils in biomolecular condensates

For introductions to biomolecular condensation and phase separation in nature and synthetic biology, two excellent reviews have been published in a special issue of *Nature Chemical Biology* (254, 255).

Physicists have been aware of the phenomenon of liquid-liquid phase separation (LLPS) for some time. More recently, biologists and chemists have shown its relevance in cell biology, where it is broadly called biomolecular condensation. In cells, this can result in membrane-less organelles (MLOs), which are responsible for sequestering and controlling a variety of subcellular processes. The key advantages over membrane-bound organelles are that MLOs can be assembled and disassembled rapidly (in seconds to minutes) and without the need for additional transcription and translation of components and that diffusion of molecules in and out of MLOs is facile. In turn, this leads to the colocalization of key biomolecules and high local concentrations of reactants to drive biochemical processes. In this way, MLOs can be direct and rapid actuators of cellular responses as needed.

Typically, the parts of natural proteins identified as being responsible for phase separation have low sequence complexity and are often assumed to be intrinsically disordered regions (IDRs). While coiled coils might be considered semi-to-low-complexity sequences, they are usually not

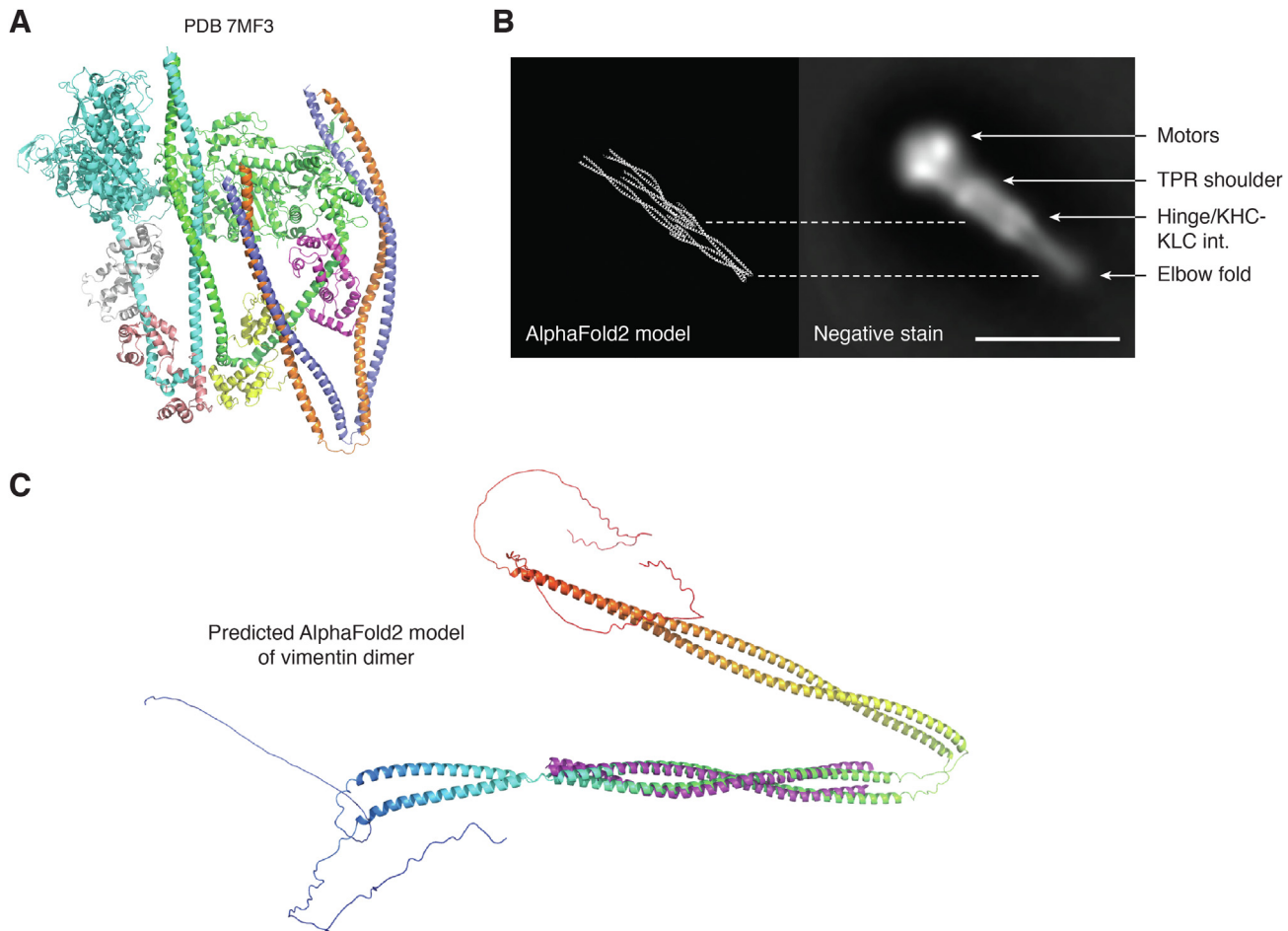


Figure 7. Large and dynamic coiled-coil assemblies. *A*, cryo-EM structure for the 10S autoinhibited state of muscle myosin-2 (7mf3, 3.4 Å) (250). Two other lower-resolution cryo-EM structures were published before this: 6xe9, 4.3 Å (249) and 6z47, 6.3 Å (248). Although the long C-terminal coiled-coil tail from the myosin heavy chains (green and cyan) is not fully resolved, these structures show how the start of this coiled coil folds back on the motor domains in the inhibited state. *B*, comparison of a back projection of the AlphaFold2 model for the coiled-coil assembly for the kinesin-1 light and heavy chains (left, low pass filtered to 30 Å) with 2D class average from experimental cryo-negative stain EM data for the autoinhibited state of full-length Kif5C/KLC1 tetramer (right) (240). Figure prepared by Dr Mark Dodding. *C*, one of the predicted AlphaFold2 models for the dimer of the human intermediate filament protein vimentin (253). Note: This is the predicted dimeric building block for much larger intermediate-filament assemblies with many thousands of protomers. The terminal regions are predicted as disordered by AlphaFold2, but only one pose is shown here, which is a simplification. The single X-ray crystal structure for a fragment of this protein is shown in purple, 1gk4 (292). Chain colored in chainbows, blue to red from the *N* to *C* termini. Figure prepared by Dr Bram Mylemans.

considered IDRs. [Although there are examples of coiled-coil predictions within IDRs and *vice versa* (20, 256, 257).] Therefore, why consider structurally defined coiled coils in biomolecular condensation? Well, recent experiments suggest that coiled coils may participate in biomolecular condensation and LLPS (258–264).

For example, in *Arabidopsis*, the coiled coil-containing FLL2 causes phase separation of polyadenylation complexes into nuclear bodies that promote polyadenylation of mRNAs (258). And the transcriptional effector TAZ undergoes LLPS via its coiled-coil domain in the nucleus of human breast cancer cells to recruit transcription machinery and promote gene expression (261). Moving out of the nucleus, the coiled-coil golgi protein GM130 and other members of the golgin family have been shown to undergo LLPS *in vitro* and when overexpressed in HeLa cells (262, 265). The scaffolding protein pericentrin is involved in centrosome expansion at the onset of mitosis. Pericentrin is long and contains many highly

conserved low complexity and coiled-coil regions. Interactions between these have been shown to lead to biomolecular condensation in centrosome maturation (263).

In all of these studies, coiled-coil domains are implicated in phase separation through biochemical studies (coiled-coil disruption/deletion), so they need to be verified structurally. However, one example where structural information is available does not necessarily shed light on these phenomena. The human PDZ- and coiled coil-containing protein harmonin from the sensory cells of the inner ear and retina undergoes LLPS at high concentrations *in vitro*. Solution-phase experiments and an X-ray crystal structure hints that harmonin's C terminus potentially forms an antiparallel coiled-coil dimer (264). However, the authors propose that coiled-coil formation is probably a consequence rather than a cause of LLPS. Clearly, we have a lot to learn about how coiled coils engage (or not) in biomolecular condensation and whether we can use them in the construction of artificial phase-separating systems (255).

Membrane-associated and transmembrane coiled-coil proteins

This perspective has focused on water-soluble and fibrous coiled-coil systems. However, there are examples of membrane-associated and membrane-spanning coiled-coil domains. In my view, these will become an increasingly rich area for coiled-coil structural and cell biology.

One of the first high-resolution coiled-coil structures was for influenza hemagglutinin (45), Figure 1. Influenza virus enters eukaryotic cells by endocytosis initiated by the HA1 domain (upper region of Fig. 1C) binding to sialic acids on the cell surface (266). Subsequent lowering of endosomal pH triggers a switch in hemagglutinin to an alternate quaternary structure centered on the trimeric HA2 coiled-coil domain, Figure 1D. This is possible because the hemagglutinin protein has already been primed into a metastable state through proteolytic cleavage of the sequence between the HA1 and HA2 domains. The quaternary rearrangement promotes fusion of the viral and host membranes, leading to release of the viral genome into the cell. This is now well understood structurally and documented in the literature and textbooks (46–49).

The eukaryotic SNARE and related proteins involved in intracellular vesicular trafficking also promote membrane fusion, though through a very different mechanism (267–270). Essentially, different components of the SNARE complex reside on different membranes. Alone, these proteins are intrinsically disordered, but when combined, they form 4-helix coiled coils. The folding and assembly brings the target membranes together and reduces the barrier to membrane fusion and subsequent mixing of the vesicular contents. This principle has been exploited to drive membrane fusion in a variety of synthetic and biological membrane systems by Kros et al. (127, 128).

Turning to proteins that traverse the membrane, there are several examples where coiled coils play interesting functional roles. I have already mentioned the α HB structures of *E. coli* Wza (244) and the F₁F₀ ATP synthase (104), Figure 5, E and G. The octameric barrel of Wza is interesting as this is a different solution to spanning the outer bacterial membrane than seeing the abundant β -porin-based domains, as seen in TolC, Figure 5D (103). Wza has inspired the design of a peptide-based ion channel (271). Smaller transmembrane barrels include the ion channel phospholamban, which is a pentamer as shown by a combined solution and solid-state NMR structure determined in lipid bilayers, Figure 5H (272). Interestingly, DeGrado has used design rules garnered for water-soluble α HBS (34) to engineer a stabilized variant of phospholamban leading to an X-ray crystal structure in micelles, 6mqu (218).

Fascinating examples of coiled-coil structural cell biology are found in the histidine kinases. These are modular, membrane-spanning proteins involved in various functions including sensing and chemotaxis in bacteria and signal transduction in eukaryotes. One of the components are the HAMP domains, which are antiparallel 4-helix coiled coils. Although several mechanisms for signal transduction by these domains have been proposed, structural studies of an archaeal HAMP suggest that a ‘gearbox’ mechanism could be a play in which alternate coiled-coil core-packing arrangements drive

the helices to rotate about their long axes to generate a rotational signal that is passed to the intracellular components (273). This area is not without its controversy, however, and Hartmann provides a more detailed review of the different proteins, alternative mechanisms, and the overall biology (241). While on altered and dynamic packing arrangements in natural coiled coils, I should mention Ghosh’s work on the surface-associated M proteins of *Streptococcus pyogenes* (Strep A) (274). These proteins disable human immunity by interacting with certain host proteins. A recent study reveals how the dimeric coiled coil of one M protein opens up to accommodate a human antimicrobial peptide in a heteromeric 3-helix bundle (275).

I would like to finish with an example of a coiled coil as a molecular ruler (276). Gram-positive bacteria present lipopolysaccharides on the outside of their outer membranes. These are essential for cell viability and involved in pathogenicity. In *E. coli* serotype 09a, two proteins appear responsible for the polymerization of the polysaccharide component with a narrow length distribution: WbdA is the polymerase and WbdD is the terminator. These form a complex with a WbdD trimer N-terminally anchored in the membrane, WbdA associated with this proximal to the membrane, and the active domains of the two proteins separated by a C-terminal trimeric coiled coil of WbdD. Although the complete coiled coil has not been resolved, its structure and function have been deciphered convincingly through a combination of X-ray crystallography, modeling, biophysical measurements (SAXS and CD spectroscopy), and functional studies with rationally truncated and extended versions of the coiled coil (276). Together, these indicate that this region is responsible for setting the length of the polysaccharide. In effect, the coiled coil acts as a rigid-rod molecular ruler that measures out the polymerizing polysaccharide until the kinase active site of WbdD is reached and polymerization is terminated.

Conclusion and outlook

My aim in writing this perspective was to capture what we have learned about the physics, chemistry, and biology of coiled-coil peptide and protein assemblies over the past half century or so. To close, I’ll give some examples of where I feel these areas are heading.

Firstly, regarding the physics and chemistry: *are the coiled-coil folding and design problems solved?* I would say, *almost*. The physical, parametric problem of backbone generation is clearly solved, and the chemical (sequence-to-structure relationship) problem is well on the way to being completed. That said, there are tripwires, and we still have some way to go to solve the coiled-coil folding and design problems fully. Most notably, despite the methods and heuristics for coiled-coil prediction, modeling, and design, we do not understand the chemical physics of how multiple weak noncovalent interactions conspire to specify and stabilize folded proteins well enough to calculate accurate energies for coiled-coil assemblies *in silico*. This is a general problem in *de novo* protein folding, assembly, and design, and the development of better

physical forcefields to model these is an ongoing and essential problem to tackle. Furthermore, with a few exceptions, successful *de novo*-designed coiled-coil peptides and proteins tend to be hyperthermal stable—in short, we have learnt to design them too well. This problem cannot be brushed under the carpet. We know that for natural proteins, thermal and chemical stabilities are limited to what is sufficient for function, that they are dynamic, and that they are turned over (rapidly if needed) by the cell. Therefore, protein designers and engineers must embrace this and deliver *de novo* proteins that are less stable, dynamic, and can be turned over as needed.

Secondly, this leads me onto the biology of coiled coils. While much of our physical and chemical understanding of coiled coils has come from studying the sequences and structures of natural coiled coils, many have regarded these as straightforward model systems from which we can learn the principles of protein structure, *mea culpa*. As we are discovering, however, natural coiled coils are much more rich, complicated, and interesting than this, and it is time for more of us to examine them in the wider context of the biological functions that they contribute to. The last section of this perspective attempted to give a glimpse of this, but there is a lot more that I have missed out. Some of the gaps in our knowledge of model and synthetic coiled-coil systems overlap with those that need exploring in intact natural coiled coils; for instance, coiled-coil dynamics and conformational switching. Others gaps will be very different: for example, *how do potentially thousands of different coiled-coil repeat proteins (some of them with very long coiled coils) avoid promiscuous interactions in the cell?* Possibilities here include nature's inclusion of nonheptad sequence repeats (55, 56) and so-called trigger sequences for folding (277–279). I am sure that new discoveries on natural coiled coils will continue to surprise us. Moreover, I contend that the amassed physical and chemical understanding of coiled-coil folding, structure, and stability will be extremely useful in improving our understanding of sequence-to-structure/function relationships of natural coiled coils *in situ*. Indeed, we are already witnessing this with the combined application of modeling (increasingly using AlphaFold2) to generate hypotheses, protein chemistry, and molecular biology to design mutants and protein fusions, advanced light microscopy to track them in cells, and cryo-EM to determine structures *in situ*. In short, advancing our physical, chemical, and biological understanding of coiled coils necessarily go hand in hand.

Thirdly, this brings me to applications or the biotechnology of coiled coils. A broadly important area is the rational and computational design of peptides that can intervene in natural peptide/protein–protein interactions (280, 281). Regarding coiled coils, progress is being made here by grafting hotspot residues from natural protein–protein interactions onto natural and *de novo*-designed coiled-coil peptides (173, 282) and by using *de novo*-designed, single-chain coiled coils (“Alpha-bodies”) to present binding-site libraries (283). These studies are mostly *in vitro*. However, recent reports show considerable promise for making *de novo* coiled-coil peptides and proteins that penetrate mammalian cells to seek out and bind specified targets (162, 284). General approaches for designing and

producing peptides/proteins that can act as exogenous reagents to target, label, and even disrupt endogenous proteins and subcellular processes would impact on protein design, cell biology, and biotechnology. Of course, along with other challenges (280, 281), rigid coiled-coil scaffolds may not be optimal for binding. Therefore, there is a pressing need to ‘soften’ and diversify coiled-coil modules as scaffolds for this approach. That said, the variety of such modules being discovered and delivered provide good starting points for such studies. This will raise other challenges, such as whether or not the *de novo*-designed binding peptides and proteins are fully orthogonal to the entire proteome of a targeted organism. But these will be fun and exciting challenges to tackle.

In summary, studying the physics and chemistry of coiled-coil proteins has been incredibly rich and rewarding. In my view, it has given us possibly the best physico-chemical understanding of any protein structure to date. Although, more broadly on repeat proteins, the work of Kajava, Regan, Plückthun, and Baker has led to similar levels of understanding and abilities to design other classes of such proteins. I have not touched on this in my perspective, but there are excellent reviews from these groups (110, 111, 285–287). All of these endeavors have delivered the means, methods, and ability to study coiled coils from atoms through to biological function. However, in my view, these physico-chemical studies are nearing completion, and it is time to reemphasize the study of coiled coils in biological contexts. This should give us a more holistic view and understanding of this ubiquitous class of protein fold. That is not to say the chemistry and physics are completely done. On the contrary, as we uncover more fascinating coiled-coil functions, full mechanistic understandings of these will be required. The emerging combination of computational modeling, protein chemistry, and high-resolution light and EM in cells puts us in a very strong position to do this. Therefore, the future of coiled-coil research is looking very exciting indeed.

Acknowledgments—D. N. W. thanks Mark Dodding for helpful discussions on motor proteins, Prasun Kumar for analysis of the CC+ database, Bram Mylemans with assistance in applying AlphaFold2, and his group members past and present who have helped to formulate and develop many of the ideas and understanding presented in this perspective.

Funding and additional information—D. N. W. is supported by grants from the Biotechnology and Biological Sciences Research Council (BBSRC): BB/S002820/1; BB/V004220/1; and BB/V006231/1. D. N. W. is also grateful to the University of Bristol for supporting the Max Planck-Bristol Centre for Minimal Biology, the BBSRC for funding the BrisSynBio (BB/L01386X/1) and BrisEngBio (BB/W013959/1) research centers, and the Royal Society for a Wolfson Research Merit Award (WM140008).

Conflict of interest—The authors declare that they have no conflicts of interest with the contents of this article.

Abbreviations—The abbreviations used are: α HB, α -helical barrel; CPA, core-packing angle; IDR, intrinsically disordered region; IF,

intermediate filament; KIH, knobs-into-holes; LLPS, liquid-liquid phase separation; MLO, membrane-less organelle; PDB, Protein Data Bank.

References

1. AlQuraishi, M. (2019) AlphaFold at CASP13. *Bioinformatics* **35**, 4862–4865
2. Baek, M., DiMaio, F., Anishchenko, I., Dauparas, J., Ovchinnikov, S., Lee, G. R., et al. (2021) Accurate prediction of protein structures and interactions using a three-track neural network. *Science* **373**, 871–876
3. Jumper, J., Evans, R., Pritzel, A., Green, T., Figurnov, M., Ronneberger, O., et al. (2021) Highly accurate protein structure prediction with AlphaFold. *Nature* **596**, 583–589
4. Varadi, M., Anyango, S., Deshpande, M., Nair, S., Natassia, C., Yordanova, G., et al. (2022) AlphaFold protein structure database: massively expanding the structural coverage of protein-sequence space with high-accuracy models. *Nucl. Acids Res.* **50**, D439–D444
5. Landschulz, W. H., Johnson, P. F., and McKnight, S. L. (1988) The leucine zipper - a hypothetical structure common to a new class of DNA-binding proteins. *Science* **240**, 1759–1764
6. O'Shea, E. K., Klemm, J. D., Kim, P. S., and Alber, T. (1991) X-ray structure of the GCN4 leucine zipper, a 2-stranded, parallel coiled coil. *Science* **254**, 539–544
7. O'Shea, E. K., Rutkowski, R., and Kim, P. S. (1989) Evidence that the leucine zipper is a coiled coil. *Science* **243**, 538–542
8. Lupas, A. (1996) Coiled coils: new structures and new functions. *Trends Biochem. Sci.* **21**, 375–382
9. Mason, J. M., and Arndt, K. M. (2004) Coiled coil domains: stability, specificity, and biological implications. *ChemBioChem* **5**, 170–176
10. Burkhard, P., Stetefeld, J., and Strelkov, S. V. (2001) Coiled coils: a highly versatile protein folding motif. *Trends Cell Biol.* **11**, 82–88
11. Rose, A., and Meier, I. (2004) Scaffolds, levers, rods and springs: diverse cellular functions of long coiled-coil proteins. *Cell Mol. Life Sci.* **61**, 1996–2009
12. Woolfson, D. N. (2005) The design of coiled-coil structures and assemblies. *Adv. Protein Chem.* **70**, 79–112
13. Lupas, A. N., and Bassler, J. (2017) Coiled coils - a model system for the 21st century. *Trends Biochem. Sci.* **42**, 130–140
14. Woolfson, D. N. (2017) Coiled-coil design: updated and upgraded. *Subcell Biochem.* **82**, 35–61
15. Lapenta, F., Aupic, J., Strmsek, Z., and Jerala, R. (2018) Coiled coil protein origami: from modular design principles towards biotechnological applications. *Chem. Soc. Rev.* **47**, 3530–3542
16. Beesley, J. L., and Woolfson, D. N. (2019) The *de novo* design of alpha-helical peptides for supramolecular self-assembly. *Curr. Opin. Biotech.* **58**, 175–182
17. Rink, W. M., and Thomas, F. (2019) De novo designed alpha-helical coiled-coil peptides as scaffolds for chemical reactions. *Chem-eur. J.* **25**, 1665–1677
18. Utterstrom, J., Naeimipour, S., Selegard, R., and Aili, D. (2021) Coiled coil-based therapeutics and drug delivery systems. *Adv. Drug Deliv. Rev.* **170**, 26–43
19. Lupas, A. N., and Gruber, M. (2005) The structure of alpha-helical coiled coils. *Adv. Protein Chem.* **70**, 37–78
20. Lupas, A. N., Bassler, J., and Dunin-Horkawicz, S. (2017) The structure and topology of alpha-helical coiled coils. *Subcell Biochem.* **82**, 95–129
21. Squire, J. M., and Parry, D. A. (2017) Fibrous protein structures: hierarchy, history and heroes. *Subcell Biochem.* **82**, 1–33
22. Crick, F. H. C. (1953) The Fourier transform of a coiled-coil. *Acta Crystallogr.* **6**, 685–689
23. Crick, F. H. C. (1953) The packing of alpha-helices - simple coiled-coils. *Acta Crystallogr.* **6**, 689–697
24. Watson, J. D., and Crick, F. H. C. (1953) Molecular structure of nucleic acids - a structure for deoxyribose nucleic acid. *Nature* **171**, 737–738
25. Pauling, L., Corey, R. B., and Branson, H. R. (1951) The structure of proteins - 2 hydrogen-bonded helical configurations of the polypeptide chain. *Proc. Natl. Acad. Sci. U. S. A.* **37**, 205–211
26. Ramachandran, G. N., Ramakrishnan, C., and Sasisekharan, V. (1963) Stereochemistry of polypeptide chain configurations. *J. Mol. Biol.* **7**, 95–99
27. Ramachandran, G. N., Venkatachalam, C. M., and Krimm, S. (1966) Stereochemical criteria for polypeptide and protein chain conformations .3. Helical and hydrogen-bonded polypeptide chains. *Biophys. J.* **6**, 849–872
28. Grigoryan, G., and DeGrado, W. F. (2011) Probing designability via a generalized model of helical bundle geometry. *J. Mol. Biol.* **405**, 1079–1100
29. Wood, C. W., Bruning, M., Ibarra, A. A., Bartlett, G. J., Thomson, A. R., Sessions, R. B., et al. (2014) CCBuilder: an interactive web-based tool for building, designing and assessing coiled-coil protein assemblies. *Bioinformatics* **30**, 3029–3035
30. Harbury, P. B., Tidor, B., and Kim, P. S. (1995) Repacking protein cores with backbone freedom - structure prediction for coiled coils. *Proc. Natl. Acad. Sci. U. S. A.* **92**, 8408–8412
31. Offer, G., Hicks, M. R., and Woolfson, D. N. (2002) Generalized crick equations for modeling noncanonical coiled coils. *J. Struct. Biol.* **137**, 41–53
32. Dunin-Horkawicz, S., and Lupas, A. N. (2010) Measuring the conformational space of square four-helical bundles with the program samCC. *J. Struct. Biol.* **170**, 226–235
33. Huang, P. S., Oberdorfer, G., Xu, C. F., Pei, X. Y., Nannenga, B. L., Rogers, J. M., et al. (2014) High thermodynamic stability of parametrically designed helical bundles. *Science* **346**, 481–485
34. Thomson, A. R., Wood, C. W., Burton, A. J., Bartlett, G. J., Sessions, R. B., Brady, R. L., et al. (2014) Computational design of water-soluble alpha-helical barrels. *Science* **346**, 485–488
35. Wood, C. W., Heal, J. W., Thomson, A. R., Bartlett, G. J., Ibarra, A. A., Brady, R. L., et al. (2017) ISAMBARD: an open-source computational environment for biomolecular analysis, modelling and design. *Bioinformatics* **33**, 3043–3050
36. Wood, C. W., and Woolfson, D. N. (2018) CCBuilder 2.0: powerful and accessible coiled-coil modeling. *Protein Sci.* **27**, 103–111
37. Walshaw, J., and Woolfson, D. N. (2001) Socket: a program for identifying and analysing coiled-coil motifs within protein structures. *J. Mol. Biol.* **307**, 1427–1450
38. Strelkov, S. V., and Burkhard, P. (2002) Analysis of alpha-helical coiled coils with the program TWISTER reveals a structural mechanism for stutter compensation. *J. Struct. Biol.* **137**, 54–64
39. Kumar, P., and Woolfson, D. N. (2021) Socket2: a program for locating, visualizing and analyzing coiled-coil interfaces in protein structures. *Bioinformatics* **37**, 4575–4577
40. Dawson, W. M., Martin, F. J. O., Rhys, G. G., Shelley, K. L., Brady, R. L., and Woolfson, D. N. (2021) Coiled coils 9-to-5: rational *de novo* design of alpha-helical barrels with tunable oligomeric states. *Chem. Sci.* **12**, 6923–6928
41. Gruber, M., and Lupas, A. N. (2003) Historical review: another 50th anniversary - new periodicities in coiled coils. *Trends Biochem. Sci.* **28**, 679–685
42. Sodek, J., Hodges, R. S., Smillie, L. B., and Jurasek, L. (1972) Amino-acid sequence of rabbit skeletal tropomyosin and its coiled coil structure. *Proc. Natl. Acad. Sci. U. S. A.* **69**, 3800–3804
43. Phillips, G. N., Fillers, J. P., and Cohen, C. (1986) Tropomyosin crystal-structure and muscle regulation. *J. Mol. Biol.* **192**, 111–128
44. Whitby, F. G., and Phillips, G. N. (2000) Crystal structure of tropomyosin at 7 Angstroms resolution. *Proteins* **38**, 49–59
45. Wilson, I. A., Skehel, J. J., and Wiley, D. C. (1981) Structure of the hemagglutinin membrane glycoprotein of influenza-virus at 3-a resolution. *Nature* **289**, 366–373
46. Bullough, P. A., Hughson, F. M., Skehel, J. J., and Wiley, D. C. (1994) Structure of influenza hemagglutinin at the pH of membrane-fusion. *Nature* **371**, 37–43

47. Carr, C. M., and Kim, P. S. (1993) A spring-loaded mechanism for the conformational change of influenza hemagglutinin. *Cell* **73**, 823–832
48. Skehel, J. J., and Wiley, D. C. (2000) Receptor binding and membrane fusion in virus entry: the influenza hemagglutinin. *Annu. Rev. Biochem.* **69**, 531–569
49. Gamblin, S. J., and Skehel, J. J. (2010) Influenza hemagglutinin and neuraminidase membrane glycoproteins. *J. Biol. Chem.* **285**, 28403–28409
50. Testa, O. D., Moutevelis, E., and Woolfson, D. N. (2009) CC plus: a relational database of coiled-coil structures. *Nucl. Acids Res.* **37**, D315–D322
51. Woolfson, D. N. (2021) A brief history of *de novo* protein design: minimal, rational, and computational. *J. Mol. Biol.* **433**, 167160
52. Kumar, P., Paterson, N. G., Clayden, J., and Woolfson, D. N. (2022) *De novo* design of discrete, stable 310-helix peptide assemblies. *Nature* **607**, 387–392
53. Kuster, D. J., Liu, C. Y., Fang, Z., Ponder, J. W., and Marshall, G. R. (2015) High-resolution crystal structures of protein helices reconciled with three-centered hydrogen bonds and multipole electrostatics. *PLoS One* **10**, e0123146
54. Pauling, L., and Corey, R. B. (1951) The structure of synthetic poly-peptides. *Proc. Natl. Acad. Sci. U. S. A.* **37**, 241–250
55. Brown, J. H., Cohen, C., and Parry, D. A. D. (1996) Heptad breaks in alpha-helical coiled coils: stutters and stammers. *Proteins-Struct. Funct. Genet.* **26**, 134–145
56. Hicks, M. R., Holberton, D. V., Kowalczyk, C., and Woolfson, D. N. (1997) Coiled-coil assembly by peptides with non-heptad sequence motifs. *Fold Des.* **2**, 149–158
57. Harbury, P. B., Plecs, J. J., Tidor, B., Alber, T., and Kim, P. S. (1998) High-resolution protein design with backbone freedom. *Science* **282**, 1462–1467
58. Hicks, M. R., Walshaw, J., and Woolfson, D. N. (2002) Investigating the tolerance of coiled-coil peptides to nonheptad sequence inserts. *J. Struct. Biol.* **137**, 73–81
59. Gabler, F., Nam, S. Z., Till, S., Mirdita, M., Steinegger, M., Soding, J., et al. (2020) Protein sequence analysis using the MPI bioinformatics toolkit. *Curr. Protoc. Bioinform.* **72**, e108
60. Lupas, A., Vandyke, M., and Stock, J. (1991) Predicting coiled coils from protein sequences. *Science* **252**, 1162–1164
61. Ludwiczak, J., Winski, A., Szczepaniak, K., Alva, V., and Dunin-Horkawicz, S. (2019) DeepCoil-a fast and accurate prediction of coiled-coil domains in protein sequences. *Bioinformatics* **35**, 2790–2795
62. Delorenzi, M., and Speed, T. (2002) An HMM model for coiled-coil domains and a comparison with PSSM-based predictions. *Bioinformatics* **18**, 617–625
63. Vincent, T. L., Green, P. J., and Woolfson, D. N. (2013) LOGICOIL—multi-state prediction of coiled-coil oligomeric state. *Bioinformatics* **29**, 69–76
64. Trigg, J., Gutwin, K., Keating, A. E., and Berger, B. (2011) Multicoil2: predicting coiled coils and their oligomerization states from sequence in the twilight zone. *PLoS One* **6**, e23519
65. Ljubetic, A., Lapenta, F., Gradišar, H., Drobnak, I., Aupic, J., Strmsek, Z., et al. (2017) Design of coiled-coil protein-origami cages that self-assemble *in vitro* and *in vivo*. *Nat. Biotechnol.* **35**, 1094–1101
66. Burley, S. K., Bhikadiya, C., Bi, C. X., Bittrich, S., Chen, L., Crichlow, G. V., et al. (2022) RCSB Protein Data Bank: celebrating 50 years of the PDB with new tools for understanding and visualizing biological macromolecules in 3D. *Protein Sci.* **31**, 187–208
67. Moutevelis, E., and Woolfson, D. N. (2009) A periodic table of coiled-coil protein structures. *J. Mol. Biol.* **385**, 726–732
68. Heal, J. W., Bartlett, G. J., Wood, C. W., Thomson, A. R., and Woolfson, D. N. (2018) Applying graph theory to protein structures: an atlas of coiled coils. *Bioinformatics* **34**, 3316–3323
69. Szczepaniak, K., Bukala, A., Neto, A. M. D., Ludwiczak, J., and Dunin-Horkawicz, S. (2020) A library of coiled-coil domains: from regular bundles to peculiar twists. *Bioinformatics* **36**, 5368–5376
70. Korendovych, I. V., and DeGrado, W. F. (2020) *De novo* protein design, a retrospective. *Q. Rev. Biophys.* **53**, e3
71. Chothia, C., Levitt, M., and Richardson, D. (1981) Helix to helix packing in proteins. *J. Mol. Biol.* **145**, 215–250
72. Baker, E. G., Bartlett, G. J., Goff, K. L. P., and Woolfson, D. N. (2017) Miniprotein design: past, present, and prospects. *Acc. Chem. Res.* **50**, 2085–2092
73. Harbury, P. B., Zhang, T., Kim, P. S., and Alber, T. (1993) A switch between 2-stranded, 3-stranded and 4-stranded coiled coils in Gcn4 leucine-zipper mutants. *Science* **262**, 1401–1407
74. Harbury, P. B., Kim, P. S., and Alber, T. (1994) Crystal-structure of an isoleucine-zipper trimer. *Nature* **371**, 80–83
75. Woolfson, D. N., and Alber, T. (1995) Predicting oligomerization states of coiled coils. *Protein Sci.* **4**, 1596–1607
76. Conway, J. F., and Parry, D. A. D. (1990) Structural features in the heptad substructure and longer range repeats of 2-stranded alpha-fibrous proteins. *Int. J. Biol. Macromol.* **12**, 328–334
77. Conway, J. F., and Parry, D. A. D. (1991) 3-Stranded alpha-fibrous proteins - the heptad repeat and its implications for structure. *Int. J. Biol. Macromol.* **13**, 14–16
78. Acharya, A., Ruvinov, S. B., Gal, J., Moll, J. R., and Vinson, C. (2002) A heterodimerizing leucine zipper coiled coil system for examining the specificity of a position interactions: amino acids I, V, L, N, A, and K. *Biochemistry* **41**, 14122–14131
79. Acharya, A., Rishi, V., and Vinson, C. (2006) Stability of 100 homo and heterotypic coiled-coil a-a' pairs for ten amino acids (A, L, I, V, N, K, S, T, E, and R). *Biochemistry* **45**, 11324–11332
80. Zhou, W. J., Smidlehner, T., and Jerala, R. (2020) Synthetic biology principles for the design of protein with novel structures and functions. *FEBS Lett.* **594**, 2199–2212
81. Liu, J., Yong, W., Deng, Y. Q., Kallenbach, N. R., and Lu, M. (2004) Atomic structure of a tryptophan-zipper pentamer. *Proc. Natl. Acad. Sci. U. S. A.* **101**, 16156–16161
82. Spencer, R. K., and Hochbaum, A. I. (2016) X-Ray crystallographic structure and solution behavior of an antiparallel coiled-coil hexamer formed by *de novo* peptides. *Biochemistry* **55**, 3214–3223
83. Spencer, R. K., and Hochbaum, A. I. (2017) The phe-ile zipper: a specific interaction motif drives antiparallel coiled-coil hexamer formation. *Biochemistry* **56**, 5300–5308
84. Rhys, G. G., Dawson, W. M., Beesley, J. L., Martin, F. J. O., Brady, R. L., Thomson, A. R., et al. (2021) How coiled-coil assemblies accommodate multiple aromatic residues. *Biomacromolecules* **22**, 2010–2019
85. Stetefeld, J., Jenny, M., Schulthess, T., Landwehr, R., Engel, J., and Kammerer, R. A. (2000) Crystal structure of a naturally occurring parallel right-handed coiled coil tetramer. *Nat. Struct. Biol.* **7**, 772–776
86. Gonzalez, L., Woolfson, D. N., and Alber, T. (1996) Buried polar residues and structural specificity in the GCN4 leucine zipper. *Nat. Struct. Biol.* **3**, 1011–1018
87. Lumb, K. J., and Kim, P. S. (1995) A buried polar interaction imparts structural uniqueness in a designed heterodimeric coiled-coil. *Biochemistry* **34**, 8642–8648
88. Thomas, F., Niitsu, A., Oregoni, A., Bartlett, G. J., and Woolfson, D. N. (2017) Conformational dynamics of asparagine at coiled-coil interfaces. *Biochemistry* **56**, 6544–6554
89. Fletcher, J. M., Boyle, A. L., Bruning, M., Bartlett, G. J., Vincent, T. L., Zaccai, N. R., et al. (2012) A basis set of *de novo* coiled-coil peptide oligomers for rational protein design and synthetic biology. *Acs Synth. Biol.* **1**, 240–250
90. Hartmann, M. D., Ridderbusch, O., Zeth, K., Albrecht, R., Testa, O., Woolfson, D. N., et al. (2009) A coiled-coil motif that sequesters ions to the hydrophobic core. *Proc. Natl. Acad. Sci. U. S. A.* **106**, 16950–16955
91. Gradišar, H., and Jerala, R. (2011) *De novo* design of orthogonal peptide pairs forming parallel coiled-coil heterodimers. *J. Pept. Sci.* **17**, 100–106
92. Thomas, F., Boyle, A. L., Burton, A. J., and Woolfson, D. N. (2013) A set of *de novo* designed parallel heterodimeric coiled coils with quantified dissociation constants in the micromolar to sub-nanomolar regime. *J. Am. Chem. Soc.* **135**, 5161–5166
93. Crooks, R. O., Lathbridge, A., Panek, A. S., and Mason, J. M. (2017) Computational prediction and design for creating iteratively larger heterospecific coiled coil sets. *Biochemistry* **56**, 1573–1584

94. Plaper, T., Aupic, J., Dekleva, P., Lapenta, F., Keber, M. M., Jerala, R., et al. (2021) Coiled-coil heterodimers with increased stability for cellular regulation and sensing SARS-CoV-2 spike protein-mediated cell fusion. *Sci. Rep.* **11**, 9136
95. Boyken, S. E., Chen, Z. B., Groves, B., Langan, R. A., Oberdorfer, G., Ford, A., et al. (2016) *De novo* design of protein homo-oligomers with modular hydrogen-bond network-mediated specificity. *Science* **352**, 680–687
96. Walshaw, J., and Woolfson, D. N. (2003) Extended knobs-into-holes packing in classical and complex coiled-coil assemblies. *J. Struct. Biol.* **144**, 349–361
97. Walshaw, J., and Woolfson, D. N. (2001) Open-and-shut cases in coiled-coil assembly: alpha-sheets and alpha-cylinders. *Protein Sci.* **10**, 668–673
98. Dunker, A. K., and Zaleske, D. J. (1977) Stereochemical considerations for constructing alpha-helical protein bundles with particular application to membrane proteins. *Biochem. J.* **163**, 45–57
99. North, B., Summa, C. M., Ghirlanda, G., and DeGrado, W. F. (2001) D-n-symmetrical tertiary templates for the design of tubular proteins. *J. Mol. Biol.* **311**, 1081–1090
100. Zaccai, N. R., Chi, B., Thomson, A. R., Boyle, A. L., Bartlett, G. J., Bruning, M., et al. (2011) *De novo* peptide hexamer with a mutable channel. *Nat. Chem. Biol.* **7**, 935–941
101. Calladine, C. R., Sharff, A., and Luisi, B. (2001) How to untwist an alpha-helix: structural principles of an alpha-helical barrel. *J. Mol. Biol.* **305**, 603–618
102. Walshaw, J., Shipway, J. M., and Woolfson, D. N. (2001) Guidelines for the assembly of novel coiled-coil structures: alpha-sheets and alpha-cylinders. *Biochem. Soc. Symp.* **68**, 111–123
103. Koronakis, V., Sharff, A., Koronakis, E., Luisi, B., and Hughes, C. (2000) Crystal structure of the bacterial membrane protein TolC central to multidrug efflux and protein export. *Nature* **405**, 914–919
104. Murphy, B. J., Klusch, N., Langer, J., Mills, D. J., Yildiz, O., and Kuhlbrandt, W. (2019) Rotary substates of mitochondrial ATP synthase reveal the basis of flexible F-1-F-o coupling. *Science* **364**, eaaw9128
105. Egelman, E. H., Xu, C., DiMaio, F., Magnotti, E., Modlin, C., Yu, X., et al. (2015) Structural plasticity of helical nanotubes based on coiled-coil assemblies. *Structure* **23**, 280–289
106. Magnotti, E. L., Hughes, S. A., Dillard, R. S., Wang, S. Y., Hough, L., Karumbamkandathil, A., et al. (2016) Self-assembly of an alpha-helical peptide into a crystalline two-dimensional nanoporous framework. *J. Am. Chem. Soc.* **138**, 16274–16282
107. Wang, F. B., Gnewou, O., Modlin, C., Beltran, L. C., Xu, C. F., Su, Z. L., et al. (2021) Structural analysis of cross alpha-helical nanotubes provides insight into the designability of filamentous peptide nanomaterials. *Nat. Commun.* **12**, 407
108. Miller, J. G., Hughes, S. A., Modlin, C., and Conticello, V. P. (2022) Structures of synthetic helical filaments and tubes based on peptide and peptido-mimetic polymers. *Q. Rev. Biophys.* **55**, e2
109. Rhys, G. G., Wood, C. W., Beesley, J. L., Zaccai, N. R., Burton, A. J., Brady, R. L., et al. (2019) Navigating the structural landscape of *de novo* alpha-helical bundles. *J. Am. Chem. Soc.* **141**, 8787–8797
110. Regan, L., Caballero, D., Hinrichsen, M. R., Virrueta, A., Williams, D. M., and O'Hern, C. S. (2015) Protein design: past, present, and future. *Biopolymers* **104**, 334–350
111. Huang, P. S., Boyken, S. E., and Baker, D. (2016) The coming of age of *de novo* protein design. *Nature* **537**, 320–327
112. Pan, X. J., and Kortemme, T. (2021) Recent advances in *de novo* protein design: principles, methods, and applications. *J. Biol. Chem.* **296**, 100558
113. Oshaben, K. M., Salari, R., McCaslin, D. R., Chong, L. T., and Horne, W. S. (2012) The native GCN4 leucine-zipper domain does not uniquely specify a dimeric oligomerization state. *Biochemistry* **51**, 9581–9591
114. Bromley, E. H. C., Channon, K., Moutevelis, E., and Woolfson, D. N. (2008) Peptide and protein building blocks for synthetic biology: from programming biomolecules to self-organized biomolecular systems. *ACS Chem. Biol.* **3**, 38–50
115. Boyle, A. L., Bromley, E. H. C., Bartlett, G. J., Sessions, R. B., Sharp, T. H., Williams, C. L., et al. (2012) Squaring the circle in peptide assembly: from fibers to discrete nanostructures by *de novo* design. *J. Am. Chem. Soc.* **134**, 15457–15467
116. O'Shea, E. K., Lumb, K. J., and Kim, P. S. (1993) Peptide Velcro - design of a heterodimeric coiled-coil. *Curr. Biol.* **3**, 658–667
117. Litowski, J. R., and Hodges, R. S. (2001) Designing heterodimeric two-stranded alpha-helical coiled-coils: the effect of chain length on protein folding, stability and specificity. *J. Pept. Res.* **58**, 477–492
118. Litowski, J. R., and Hodges, R. S. (2002) Designing heterodimeric two-stranded alpha-helical coiled-coils - effects of hydrophobicity and alpha-helical propensity on protein folding, stability, and specificity. *J. Biol. Chem.* **277**, 37272–37279
119. Edgell, C. L., Smith, A. J., Beesley, J. L., Savery, N. J., and Woolfson, D. N. (2020) *De novo* designed protein-interaction modules for in-cell applications. *Acs Synth. Biol.* **9**, 427–436
120. Nauiyal, S., Woolfson, D. N., King, D. S., and Alber, T. (1995) A designed heterotrimeric coiled-coil. *Biochemistry* **34**, 11645–11651
121. Nauiyal, S., and Alber, T. (1999) Crystal structure of a designed, thermostable; heterotrimeric coiled coil. *Protein Sci.* **8**, 84–90
122. Bermeo, S., Favor, A., Chang, Y. T., Norris, A., Boyken, S. E., Hsia, Y., et al. (2022) *De novo* design of obligate ABC-type heterotrimeric proteins. *Nat. Struct. Mol. Biol.* **29**, 1266–1276
123. Reinke, A. W., Grant, R. A., and Keating, A. E. (2010) A synthetic coiled-coil interactome provides heterospecific modules for molecular engineering. *J. Am. Chem. Soc.* **132**, 6025–6031
124. Thompson, K. E., Bashor, C. J., Lim, W. A., and Keating, A. E. (2012) SYNZIP protein interaction toolbox: *in vitro* and *in vivo* specifications of heterospecific coiled-coil interaction domains. *Acs Synth. Biol.* **1**, 118–129
125. Plaper, T., Aupic, J., Dekleva, P., Lapenta, F., Jerala, R., and Bencina, M. (2021) *De novo* designed parallel heterodimeric coiled-coil peptide pairs with high affinity for use in mammalian cells. *FEBS Open Biol.* **11**, 269
126. Lindhout, D. A., Litowski, J. R., Mercier, P., Hodges, R. S., and Sykes, B. D. (2004) NMR solution structure of a highly stable *de novo* heterodimeric coiled-coil. *Biopolymers* **75**, 367–375
127. Marsden, H. R., Elbers, N. A., Bomans, P. H. H., Sommerdijk, N. A. J. M., and Kros, A. (2009) A reduced SNARE model for membrane fusion. *Angew. Chem. Int. Edit.* **48**, 2330–2333
128. Marsden, H. R., Tomatsu, I., and Kros, A. (2011) Model systems for membrane fusion. *Chem. Soc. Rev.* **40**, 1572–1585
129. Chao, G., Wannier, T. M., Gutierrez, C., Borders, N. C., Appleton, E., Chadha, A., et al. (2022) helixCAM: a platform for programmable cellular assembly in bacteria and human cells. *Cell* **185**, 3551–3567. e3539
130. Gradirar, H., Bozic, S., Doles, T., Vengust, D., Hafner-Bratkovic, I., Mertelj, A., et al. (2013) Design of a single-chain polypeptide tetrahedron assembled from coiled-coil segments. *Nat. Chem. Biol.* **9**, 362–366
131. Eklund, A. S., Ganji, M., Gavins, G., Seitz, O., and Jungmann, R. (2020) Peptide-PAINT super-resolution imaging using transient coiled coil interactions. *Nano Lett.* **20**, 6732–6737
132. Oi, C., Gidden, Z., Holyoake, L., Kantelberg, O., Mochrie, S., Horrocks, M. H., et al. (2020) LIVE-PAINT allows super-resolution microscopy inside living cells using reversible peptide-protein interactions. *Commun. Biol.* **3**, 458
133. Mason, J. M., Schmitz, M. A., Muller, K., and Arndt, K. M. (2006) Semirational design of Jun-Fos coiled coils with increased affinity: universal implications for leucine zipper prediction and design. *Proc. Natl. Acad. Sci. U. S. A.* **103**, 8989–8994
134. Mason, J. M., Muller, K. M., and Arndt, K. M. (2008) iPEP: peptides designed and selected for interfering with protein interaction and function. *Biochem. Soc. Trans.* **36**, 1442–1447
135. Grigoryan, G., Reinke, A. W., and Keating, A. E. (2009) Design of protein-interaction specificity gives selective bZIP-binding peptides. *Nature* **458**, 859–864
136. Reinke, A. W., Grigoryan, G., and Keating, A. E. (2010) Identification of bZIP interaction partners of viral proteins HBZ, MEQ, BZLF1, and K-bZIP using coiled-coil arrays. *Biochemistry* **49**, 1985–1997

137. Potapov, V., Kaplan, J. B., and Keating, A. E. (2015) Data-driven prediction and design of bZIP coiled-coil interactions. *PLoS Comput. Biol.* **11**, e1004046
138. Liu, J., Zheng, Q., Deng, Y. Q., Cheng, C. S., Kallenbach, N. R., and Lu, M. (2006) A seven-helix coiled coil. *Proc. Natl. Acad. Sci. U. S. A.* **103**, 15457–15462
139. Taylor, W. R., Chelliah, V., Hollup, S. M., MacDonald, J. T., and Jonassen, I. (2009) Probing the "dark matter" of protein fold space. *Structure* **17**, 1244–1252
140. Woolfson, D. N., Bartlett, G. J., Burton, A. J., Heal, J. W., Niitsu, A., Thomson, A. R., et al. (2015) *De novo* protein design: how do we expand into the universe of possible protein structures? *Curr. Opin. Struc Biol.* **33**, 16–26
141. Burton, A. J., Thomas, F., Agnew, C., Hudson, K. L., Halford, S. E., Brady, R. L., et al. (2013) Accessibility, reactivity, and selectivity of side chains within a channel of *de novo* peptide assembly. *J. Am. Chem. Soc.* **135**, 12524–12527
142. Fong, J. H., Keating, A. E., and Singh, M. (2004) Predicting specificity in bZIP coiled-coil protein interactions. *Genome Biol.* **5**, R11
143. Edgell, C. L., Savery, N. J., and Woolfson, D. N. (2020) Robust *de novo*-designed homotetrameric coiled coils. *Biochemistry* **59**, 1087–1092
144. Rhys, G. G., Wood, C. W., Lang, E. J. M., Mulholland, A. J., Brady, R. L., Thomson, A. R., et al. (2018) Maintaining and breaking symmetry in homomeric coiled-coil assemblies. *Nat. Commun.* **9**, 4132
145. Dawson, W. M., Lang, E. J. M., Rhys, G. G., Shelley, K. L., Williams, C., Brady, R. L., et al. (2021) Structural resolution of switchable states of a *de novo* peptide assembly. *Nat. Commun.* **12**, 1530
146. Bryson, J. W., Betz, S. F., Lu, H. S., Suich, D. J., Zhou, H. X. X., Oneil, K. T., et al. (1995) Protein design - a hierarchical approach. *Science* **270**, 935–941
147. Hill, R. B., Raleigh, D. P., Lombardi, A., and Degrado, W. F. (2000) *De novo* design of helical bundles as models for understanding protein folding and function. *Acc. Chem Res.* **33**, 745–754
148. [preprint] Naudin, E. A., Albanese, K. I., Smith, A. J., Mylemans, B., Baker, E. G., Weiner, O. D., et al. (2022) From peptides to proteins: coiled-coil tetramers to single-chain 4-helix bundles. *bioRxiv*. <https://doi.org/10.1101/2022.08.04.502660>
149. Regan, L., and Degrado, W. F. (1988) Characterization of a helical protein designed from 1st principles. *Science* **241**, 976–978
150. Hecht, M. H., Richardson, J. S., Richardson, D. C., and Ogden, R. C. (1990) *De novo* design, expression, and characterization of felix - a 4-helix bundle protein of native-like sequence. *Science* **249**, 884–891
151. Gernert, K. M., Surles, M. C., Labean, T. H., Richardson, J. S., and Richardson, D. C. (1995) The alacoil - a very tight, antiparallel coiled-coil of helices. *Protein Sci.* **4**, 2252–2260
152. McClain, D. L., Woods, H. L., and Oakley, M. G. (2001) Design and characterization of a heterodimeric coiled coil that forms exclusively with an antiparallel relative helix orientation. *J. Am. Chem. Soc.* **123**, 3151–3152
153. Gurnon, D. G., Whitaker, J. A., and Oakley, M. G. (2003) Design and characterization of a homodimeric antiparallel coiled coil. *J. Am. Chem. Soc.* **125**, 7518–7519
154. Negron, C., and Keating, A. E. (2014) A set of computationally designed orthogonal antiparallel homodimers that expands the synthetic coiled-coil toolkit. *J. Am. Chem. Soc.* **136**, 16544–16556
155. Monera, O. D., Zhou, N. E., Kay, C. M., and Hodges, R. S. (1993) Comparison of antiparallel and parallel 2-stranded alpha-helical coiled-coils - design, synthesis, and characterization. *J. Biol. Chem.* **268**, 19218–19227
156. Monera, O. D., Kay, C. M., and Hodges, R. S. (1994) Electrostatic interactions control the parallel and antiparallel orientation of alpha-helical chains in 2-stranded alpha-helical coiled-coils. *Biochemistry* **33**, 3862–3871
157. Oakley, M. G., and Hollenbeck, J. J. (2001) The design of antiparallel coiled coils. *Curr. Opin. Struc Biol.* **11**, 450–457
158. Hadley, E. B., Testa, O. D., Woolfson, D. N., and Gellman, S. H. (2008) Preferred side-chain constellations at antiparallel coiled-coil interfaces. *Proc. Natl. Acad. Sci. U. S. A.* **105**, 530–535
159. Steinkruger, J. D., Bartlett, G. J., Hadley, E. B., Fay, L., Woolfson, D. N., and Gellman, S. H. (2012) The d'-d-d' vertical triad is less discriminating than the a'-a-a' vertical triad in the antiparallel coiled-coil dimer motif. *J. Am. Chem. Soc.* **134**, 2626–2633
160. Majerle, A., Hadzi, S., Aupic, J., Satler, T., Lapenta, F., Strmsek, Z., et al. (2021) A nanobody toolbox targeting dimeric coiled-coil modules for functionalization of designed protein origami structures. *Proc. Natl. Acad. Sci. U. S. A.* **118**, e2021899118
161. Pandya, M. J., Cerasoli, E., Joseph, A., Stoneman, R. G., Waite, E., and Woolfson, D. N. (2004) Sequence and structural duality: designing peptides to adopt two stable conformations. *J. Am. Chem. Soc.* **126**, 17016–17024
162. Rhys, G. G., Cross, J. A., Dawson, W. M., Thompson, H. F., Shanmugaratnam, S., Savery, N. J., et al. (2022) *De novo* designed peptides for cellular delivery and subcellular localisation. *Nat. Chem. Biol.* **18**, 999–1004
163. Lebar, T., Lainscek, D., Merljak, E., Aupic, J., and Jerala, R. (2020) A tunable orthogonal coiled-coil interaction toolbox for engineering mammalian cells. *Nat. Chem. Biol.* **16**, 513
164. Pandya, M. J., Spooner, G. M., Sunde, M., Thorpe, J. R., Rodger, A., and Woolfson, D. N. (2000) Sticky-end assembly of a designed peptide fiber provides insight into protein fibrilllogenesis. *Biochemistry* **39**, 8728–8734
165. Banwell, E. F., Abelardo, E. S., Adams, D. J., Birchall, M. A., Corrigan, A., Donald, A. M., et al. (2009) Rational design and application of responsive alpha-helical peptide hydrogels. *Nat. Mater.* **8**, 596–600
166. Yoshizumi, A., Fletcher, J. M., Yu, Z. X., Persikov, A. V., Bartlett, G. J., Boyle, A. L., et al. (2011) Designed coiled coils promote folding of a recombinant bacterial collagen. *J. Biol. Chem.* **286**, 17512–17520
167. Fletcher, J. M., Harniman, R. L., Barnes, F. R. H., Boyle, A. L., Collins, A., Mantell, J., et al. (2013) Self-assembling cages from coiled-coil peptide modules. *Science* **340**, 595–599
168. Beesley, J. L., Baum, H. E., Hodgson, L. R., Verkade, P., Banting, G. S., and Woolfson, D. N. (2018) Modifying self-assembled peptide cages to control internalization into mammalian cells. *Nano Lett.* **18**, 5933–5937
169. Morris, C., Glennie, S. J., Lam, H. S., Baum, H. E., Kandage, D., Williams, N. A., et al. (2019) A modular vaccine platform combining self-assembled peptide cages and immunogenic peptides. *Adv. Funct. Mater.* **29**, 1807357
170. Smith, A. J., Thomas, F., Shoemark, D., Woolfson, D. N., and Savery, N. J. (2019) Guiding biomolecular interactions in cells using *de novo* protein-protein interfaces. *ACS Synth. Biol.* **8**, 1284–1293
171. Lee, M. J., Mantell, J., Hodgson, L., Alibhai, D., Fletcher, J. M., Brown, I. R., et al. (2018) Engineered synthetic scaffolds for organizing proteins within the bacterial cytoplasm. *Nat. Chem. Biol.* **14**, 142–147
172. Jin, J., Baker, E. G., Wood, C. W., Bath, J., Woolfson, D. N., and Turberfield, A. J. (2019) Peptide assembly directed and quantified using megadalton DNA nanostructures. *ACS Nano* **13**, 9927–9935
173. Fletcher, J. M., Horner, K. A., Bartlett, G. J., Rhys, G. G., Wilson, A. J., and Woolfson, D. N. (2018) *De novo* coiled-coil peptides as scaffolds for disrupting protein-protein interactions. *Chem. Sci.* **9**, 7656–7665
174. Harrington, L., Fletcher, J. M., Heermann, T., Woolfson, D. N., and Schwille, P. (2021) *De novo* design of a reversible phosphorylation-dependent switch for membrane targeting. *Nat. Commun.* **12**, 1472
175. Anton, Z., Weijman, J. F., Williams, C., Moody, E. R. R., Mantell, J., Yip, Y. Y., et al. (2021) Molecular mechanism for kinesin-1 direct membrane recognition. *Sci. Adv.* **7**, eabgg6636
176. Burgess, N. C., Sharp, T. H., Thomas, F., Wood, C. W., Thomson, A. R., Zaccai, N. R., et al. (2015) Modular design of self-assembling peptide-based nanotubes. *J. Am. Chem. Soc.* **137**, 10554–10562
177. Thomas, F., Burgess, N. C., Thomson, A. R., and Woolfson, D. N. (2016) Controlling the assembly of coiled-coil peptide nanotubes. *Angew. Chem. Int. Edit.* **55**, 987–991
178. Xu, C. F., Liu, R., Mehta, A. K., Guerrero-Ferreira, R. C., Wright, E. R., Dunin-Horkawicz, S., et al. (2013) Rational design of helical nanotubes from self-assembly of coiled-coil lock washers. *J. Am. Chem. Soc.* **135**, 15565–15578

179. Thomas, F., Dawson, W. M., Lang, E. J. M., Burton, A. J., Bartlett, G. J., Rhys, G. G., et al. (2018) *De novo*-designed alpha-helical barrels as receptors for small molecules. *Acs Synth. Biol.* **7**, 1808–1816
180. Dawson, W. M., Shelley, K. L., Fletcher, J. M., Scott, D. A., Lombardi, L., Rhys, G. G., et al. (2023) Differential sensing with arrays of *de novo* designed peptide assemblies. *Nat. Commun.* **14**, 383
181. Scott, A. J., Niitsu, A., Kratochvil, H. T., Lang, E. J. M., Sengel, J. T., Dawson, W. M., et al. (2021) Constructing ion channels from water-soluble alpha-helical barrels. *Nat. Chem.* **13**, 643–650
182. Crooks, R. O., Baxter, D., Panek, A. S., Lubben, A. T., and Mason, J. M. (2016) Deriving heterospecific self-assembling protein-protein interactions using a computational interactome screen. *J. Mol. Biol.* **428**, 385–398
183. Moll, J. R., Ruvinov, S. B., Pastan, I., and Vinson, C. (2001) Designed heterodimerizing leucine zippers with a range of pIs and stabilities up to 10(–15) M. *Protein Sci.* **10**, 649–655
184. Aronsson, C., Danmark, S., Zhou, F., Oberg, P., Enander, K., Su, H. B., et al. (2015) Self-sorting heterodimeric coiled coil peptides with defined and tuneable self-assembly properties. *Sci. Rep.* **5**, 14063
185. Watson, M. D., Peran, I., and Raleigh, D. P. (2016) A non-perturbing probe of coiled coil formation based on electron transfer mediated fluorescence quenching. *Biochemistry* **55**, 3685–3691
186. Sztatelman, O., Kopec, K., Pedziwiatr, M., Trojnar, M., Worch, R., Wielgus-Kutrowska, B., et al. (2019) Heterodimerizing helices as tools for nanoscale control of the organization of protein-protein and protein-quantum dots. *Biochimie* **167**, 93–105
187. Fujita, S., and Matsura, K. (2017) Self-assembled artificial viral capsids bearing coiled-coils at the surface. *Org. Biomol. Chem.* **15**, 5070–5077
188. Small, L. S. R., Bruning, M., Thomson, A. R., Boyle, A. L., Davies, R. B., Curmi, P. M. G., et al. (2017) Construction of a chassis for a tripartite protein-based molecular motor. *Acs Synth. Biol.* **6**, 1096–1102
189. Groth, M. C., Rink, W. M., Meyer, N. F., and Thomas, F. (2018) Kinetic studies on strand displacement in *de novo* designed parallel heterodimeric coiled coils. *Chem. Sci.* **9**, 4308–4316
190. Tunn, I., de Leon, A. S., Blank, K. G., and Harrington, M. J. (2018) Tuning coiled coil stability with histidine-metal coordination. *Nanoscale* **10**, 22725–22729
191. Lopez-Garcia, P., Goktas, M., Bergues-Pupo, A. E., Koksich, B., Silva, D. V., and Blank, K. G. (2019) Structural determinants of coiled coil mechanics. *Phys. Chem. Chem. Phys.* **21**, 9145–9149
192. Tunn, I., Harrington, M. J., and Blank, K. G. (2019) Bioinspired histidine-Zn²⁺ coordination for tuning the mechanical properties of self-healing coiled coil cross-linked hydrogels. *Biomimetics-Basel* **4**, 25
193. Hussey, B. J., and McMillen, D. R. (2018) Programmable T7-based synthetic transcription factors. *Nucl. Acids Res.* **46**, 9842–9854
194. Mueller, C., and Grossmann, T. N. (2018) Coiled-coil peptide beacon: a tunable conformational switch for protein detection. *Angew. Chem. Int. Edit* **57**, 17079–17083
195. Trang, V. H., Zhang, X. Q., Yumul, R. C., Zeng, W. P., Stone, I. J., Wo, S. W., et al. (2019) A coiled-coil masking domain for selective activation of therapeutic antibodies. *Nat. Biotechnol.* **37**, 761–765
196. Jasaitis, L., Silver, C. D., Rawlings, A. E., Peters, D. T., Whelan, F., Regan, L., et al. (2020) Rational design and self-assembly of coiled-coil linked SasG protein fibrils. *Acs Synth. Biol.* **9**, 1599–1607
197. Cristie-David, A. S., Sciore, A., Badieyan, S., Eschweiler, J. D., Koldevey, P., Bardwell, J. C. A., et al. (2017) Evaluation of *de novo*-designed coiled coils as off-the-shelf components for protein assembly. *Mol. Syst. Des. Eng.* **2**, 140–148
198. Heckmeier, P. J., Agam, G., Teese, M. G., Hoyer, M., Stehle, R., Lamb, D. C., et al. (2020) Determining the stoichiometry of small protein oligomers using steady-state fluorescence anisotropy. *Biophys. J.* **119**, 99–114
199. Cannon, K. A., Nguyen, V. N., Morgan, C., and Yeates, T. O. (2020) Design and characterization of an icosahedral protein cage formed by a double-fusion protein containing three distinct symmetry elements. *Acs Synth. Biol.* **9**, 517–524
200. Miyamoto, T., Hayashi, Y., Yoshida, K., Watanabe, H., Uchihashi, T., Yonezawa, K., et al. (2019) Construction of a quadrangular tetramer and a cage-like hexamer from three-helix bundle-linked fusion proteins. *Acs Synth. Biol.* **8**, 1112–1120
201. Badieyan, S., Sciore, A., Eschweiler, J. D., Koldevey, P., Cristie-David, A. S., Ruotolo, B. T., et al. (2017) Symmetry-directed self-assembly of a tetrahedral protein cage mediated by *de novo*-designed coiled coils. *Chembiochem* **18**, 1888–1892
202. Sciore, A., Su, M., Koldevey, P., Eschweiler, J. D., Diffley, K. A., Linhares, B. M., et al. (2016) Flexible, symmetry-directed approach to assembling protein cages. *Proc. Natl. Acad. Sci. U. S. A.* **113**, 8681–8686
203. Swainsbury, D. J. K., Harniman, R. L., Di Bartolo, N. D., Liu, J. T., Harper, W. F. M., Corrie, A. S., et al. (2016) Directed assembly of defined oligomeric photosynthetic reaction centres through adaptation with programmable extra-membrane coiled-coil interfaces. *Biochim. Biophys. Acta* **1857**, 1829–1839
204. Sweeney, S. M., Bullen, G. A., Gillis, R. B., Adams, G. G., Rowe, A. J., Harding, S. E., et al. (2016) Coiled coil type neoglycoproteins presenting three lactose residues. *Tetrahedron Lett.* **57**, 1414–1417
205. Ramberg, K. O., Guagnini, F., Engilberge, S., Wronska, M. A., Rennie, M. L., Perez, J., et al. (2021) Segregated protein-cucurbit[7]uril crystalline architectures via modulatory peptide tectons. *Chem-eur J.* **27**, 14619–14627
206. Susjan, P., Roskar, S., and Hafner-Bratkovic, I. (2017) The mechanism of NLRP3 inflammasome initiation: trimerization but not dimerization of the NLRP3 pyrin domain induces robust activation of IL-1 beta. *Biochem. Biophys. Res. Commun.* **483**, 823–828
207. Guo, L., Bi, W. W., Wang, X. L., Xu, W., Yan, R. H., Zhang, Y. Y., et al. (2021) Engineered trimeric ACE2 binds viral spike protein and locks it in "Three-up" conformation to potently inhibit SARS-CoV-2 infection. *Cell Res.* **31**, 98–100
208. Scheib, K. A., Tavenor, N. A., Lawless, M. J., Saxena, S., and Horne, W. S. (2019) Understanding and controlling the metal-directed assembly of terpyridine-functionalized coiled-coil peptides. *Chem. Commun.* **55**, 7752–7755
209. Tavenor, N. A., Murnin, M. J., and Horne, W. S. (2017) Supramolecular metal-coordination polymers, nets, and frameworks from synthetic coiled-coil peptides. *J. Am. Chem. Soc.* **139**, 2212–2215
210. Boyle, A. L., Rabe, M., Crone, N. S. A., Rhys, G. G., Soler, N., Voskamp, P., et al. (2019) Selective coordination of three transition metal ions within a coiled-coil peptide scaffold. *Chem. Sci.* **10**, 7456–7465
211. Biok, N. A., Passow, A. D., Wang, C. X., Bingman, C. A., Abbott, N. L., and Gellman, S. H. (2019) Retention of coiled-coil dimer formation in the absence of ion pairing at positions flanking the hydrophobic core. *Biochemistry* **58**, 4821–4826
212. Szefczyk, M., Szulc, N., Gasior-Glogowska, M., Modrak-Wojcik, A., Bzowska, A., Majstrzyk, W., et al. (2021) Hierarchical approach for the rational construction of helix-containing nanofibrils using alpha,beta-peptides. *Nanoscale* **13**, 4000–4015
213. Chung, C. I., Zhang, Q., and Shu, X. K. (2018) Dynamic imaging of small molecule induced protein-protein interactions in living cells with a fluorophore phase transition based approach. *Anal. Chem.* **90**, 14287–14293
214. Zhang, Q., Huang, H., Zhang, L. Q., Wu, R., Chung, C. I., Zhang, S. Q., et al. (2018) Visualizing dynamics of cell signaling *in vivo* with a phase separation-based kinase reporter. *Mol. Cell* **69**, 334–346.e4
215. Mann, F. A., Horlebein, J., Meyer, N. F., Meyer, D., Thomas, F., and Kruss, S. (2018) Carbon nanotubes encapsulated in coiled-coil peptide barrels. *Chemistry* **24**, 12241–12245
216. Farhadi, S. A., Liu, R. J., Becker, M. W., Phelps, E. A., and Hudalla, G. A. (2021) Physical tuning of galectin-3 signaling. *Proc. Natl. Acad. Sci. U. S. A.* **118**, e2024117118
217. Anuar, I. N. A. K., Banerjee, A., Keeble, A. H., Carella, A., Nikov, G. I., and Howarth, M. (2019) Spy&Go purification of SpyTag-proteins using pseudo-SpyCatcher to access an oligomerization toolbox. *Nat. Commun.* **10**, 1734
218. Mravic, M., Thomaston, J. L., Tucker, M., Solomon, P. E., Liu, L. J., and DeGrado, W. F. (2019) Packing of apolar side chains enables accurate design of highly stable membrane proteins. *Science* **363**, 1418–1423

219. Xu, C. F., Lu, P. L., El-Din, T. M. G., Pei, X. Y., Johnson, M. C., Uyeda, A., et al. (2020) Computational design of transmembrane pores. *Nature* **585**, 129–134
220. Lim, S. I., Lukianov, C. I., and Champion, J. A. (2017) Self-assembled protein nanocarrier for intracellular delivery of antibody. *J. Control Release* **249**, 1–10
221. Dhankher, A., Hernandez, M. E., Howard, H. C., and Champion, J. A. (2020) Characterization and control of dynamic rearrangement in a self-assembled antibody carrier. *Biomacromolecules* **21**, 1407–1416
222. Dhankher, A., Lv, W., Studstill, W. T., and Champion, J. A. (2021) Coiled coil exposure and histidine tags drive function of an intracellular protein drug carrier. *J. Control Release* **339**, 248–258
223. Lv, W., and Champion, J. A. (2021) Demonstration of intracellular trafficking, cytosolic bioavailability, and target manipulation of an antibody delivery platform. *Nanomedicine* **32**, 102315
224. Guzenko, D., Chernyatina, A. A., and Strelkov, S. V. (2017) Crystallographic studies of intermediate filament proteins. *Subcell Biochem.* **82**, 151–170
225. Newman, J. R. S., and Keating, A. E. (2003) Comprehensive identification of human bZIP interactions with coiled-coil arrays. *Science* **300**, 2097–2101
226. Grigoryan, G., and Keating, A. E. (2008) Structural specificity in coiled-coil interactions. *Curr. Opin. Struc Biol.* **18**, 477–483
227. Lupas, A. (1996) Prediction and analysis of coiled-coil structures. *Met Enzymol.* **266**, 513–525
228. Newman, J. R. S., Wolf, E., and Kim, P. S. (2000) A computationally directed screen identifying interacting coiled coils from *Saccharomyces cerevisiae*. *Proc. Natl. Acad. Sci. U. S. A.* **97**, 13203–13208
229. Rose, A., Manikantan, S., Schraegle, S. J., Maloy, M. A., Stahlberg, E. A., and Meier, I. (2004) Genome-wide identification of *Arabidopsis* coiled-coil proteins and establishment of the ARABI-COIL database. *Plant Physiol.* **134**, 927–939
230. Rose, A., Schraegle, S. J., Stahlberg, E. A., and Meier, I. (2005) Coiled-coil protein composition of 22 proteomes - differences and common themes in subcellular infrastructure and traffic control. *BMC Evol Biol.* **5**, 66
231. Barbara, K. E., Willis, K. A., Haley, T. M., Deminoff, S. J., and Santangelo, G. M. (2007) Coiled coil structures and transcription: an analysis of the *S. cerevisiae* coilmome. *Mol. Genet. Genomics* **278**, 135–147
232. Rackham, O. J. L., Madera, M., Armstrong, C. T., Vincent, T. L., Woolfson, D. N., and Gough, J. (2010) The evolution and structure prediction of coiled coils across all genomes. *J. Mol. Biol.* **403**, 480–493
233. Yang, Z. M., Sun, J., Chen, Y., Zhu, P. P., Zhang, L., Wu, S. Y., et al. (2019) Genome-wide identification, structural and gene expression analysis of the bZIP transcription factor family in sweet potato wild relative *Ipomoea trifida*. *BMC Genet.* **20**, 41
234. Simm, D., Hatje, K., Waack, S., and Kollmar, M. (2021) Critical assessment of coiled-coil predictions based on protein structure data. *Sci. Rep.* **11**, 12439
235. Fontana, P., Dong, Y., Pi, X., Tong, A. B., Hecksel, C. W., Wang, L. F., et al. (2022) Structure of cytoplasmic ring of nuclear pore complex by integrative cryo-EM and AlphaFold. *Science* **376**, eabm9326
236. Fu, R. J., Su, W. P., and He, H. X. (2022) Direct phasing of coiled-coil protein crystals. *Crystals* **12**, 1674
237. Morellet, N., Hardouin, P., Assrir, N., van Heijenoort, C., and Golinelli-Pimpaneau, B. (2022) Structural insights into the dimeric form of *Bacillus subtilis* RNase Y using NMR and AlphaFold. *Biomolecules* **12**, 1798
238. Noone, D. P., Dijkstra, D. J., van Der Klugt, T. T., van Veelen, P. A., de Ru, A. H., Hensbergen, P. J., et al. (2022) PTX3 structure determination using a hybrid cryoelectron microscopy and AlphaFold approach offers insights into ligand binding and complement activation. *Proc. Natl. Acad. Sci. U. S. A.* **119**, e2208144119
239. Simpkin, A. J., Thomas, J. M. H., Keegan, R. M., and Rigden, D. J. (2022) MrParse: finding homologues in the PDB and the EBI AlphaFold database for molecular replacement and more. *Acta Crystallogr. D* **78**, 553–559
240. Weijman, J. F., Yadav, S. K. N., Surridge, K. J., Cross, J. A., Borucu, U., Mantell, J., et al. (2022) Molecular architecture of the autoinhibited kinesin-1 lambda particle. *Sci. Adv.* **8**, eabp9660
241. Hartmann, M. D. (2017) Functional and structural roles of coiled coils. *Subcell Biochem.* **82**, 63–93
242. Tunyasuvunakool, K., Adler, J., Wu, Z., Green, T., Zielinski, M., Zidek, A., et al. (2021) Highly accurate protein structure prediction for the human proteome. *Nature* **596**, 590–596
243. Malashkevich, V. N., Kammerer, R. A., Efimov, V. P., Schulthess, T., and Engel, J. (1996) The crystal structure of a five-stranded coiled coil in COMP: a prototype ion channel? *Science* **274**, 761–765
244. Dong, C. J., Beis, K., Nesper, J., Brunkan-LaMontagne, A. L., Clarke, B. R., Whitfield, C., et al. (2006) Wza the translocon for E-coli capsular polysaccharides defines a new class of membrane protein. *Nature* **444**, 226–229
245. Niitsu, A., Heal, J. W., Fauland, K., Thomson, A. R., and Woolfson, D. N. (2017) Membrane-spanning alpha-helical barrels as tractable protein-design targets. *Philos Trans. R Soc. Lond. B Biol Sci.* **372**, 20160213
246. Trivedi, D. V., Nag, S., Spudich, A., Ruppel, K. M., and Spudich, J. A. (2020) The myosin family of mechanoenzymes: from mechanisms to therapeutic approaches. *Annu. Rev. Biochem.* **89**, 667–693
247. Cason, S. E., and Holzbaur, E. L. F. (2022) Selective motor activation in organelle transport along axons. *Nat. Rev. Mol. Cell Biol.* **23**, 699–714
248. Scarff, C. A., Carrington, G., Casas-Mao, D., Chalovich, J. M., Knight, P. J., Ranson, N. A., et al. (2020) Structure of the shutdown state of myosin-2. *Nature* **588**, 515–520
249. Yang, S. X., Tiwari, P., Lee, K. H., Sato, O., Ikebe, M., Padron, R., et al. (2020) Cryo-EM structure of the inhibited (10S) form of myosin II. *Nature* **588**, 521–525
250. Heissler, S. M., Arora, A. S., Billington, N., Sellers, J. R., and Chinthalapudi, K. (2021) Cryo-EM structure of the autoinhibited state of myosin-2. *Sci. Adv.* **7**, eabk3273
251. Vermeire, P. J., Stalmans, G., Lilina, A. V., Fiala, J., Novak, P., Herrmann, H., et al. (2021) Molecular interactions driving intermediate filament assembly. *Cells* **10**, 2457
252. Meier, M., Padilla, G. P., Herrmann, H., Wedig, T., Herzt, M., Patel, T. R., et al. (2009) Vimentin coil 1A-A molecular switch involved in the initiation of filament elongation. *J. Mol. Biol.* **390**, 245–261
253. Lilina, A. V., Leekens, S., Hashim, H. M., Vermeire, P. J., Harvey, J. N., and Strelkov, S. V. (2022) Stability profile of vimentin rod domain. *Protein Sci.* **31**, e4505
254. Villegas, J. A., Heidenreich, M., and Levy, E. D. (2022) Molecular and environmental determinants of biomolecular condensate formation. *Nat. Chem. Biol.* **18**, 1319–1329
255. Qian, Z. G., Huang, S. C., and Xia, X. X. (2022) Synthetic protein condensates for cellular and metabolic engineering. *Nat. Chem. Biol.* **18**, 1330–1340
256. Szappanos, B., Sugeves, D., Nyitrai, L., Perczel, A., and Gaspari, Z. (2010) Folded-unfolded cross-predictions and protein evolution: the case study of coiled-coils. *FEBS Lett.* **584**, 1623–1627
257. Valsecchi, I., Guitard-Crilat, E., Maldiney, R., Habricot, Y., Lignon, S., Lebrun, R., et al. (2013) The intrinsically disordered C-terminal region of *Arabidopsis thaliana* TCP8 transcription factor acts both as a trans-activation and self-assembly domain. *Mol. Biosyst.* **9**, 2282–2295
258. Fang, X. F., Wang, L., Ishikawa, R., Li, Y. X., Fiedler, M., Liu, F. Q., et al. (2019) Arabidopsis FLL2 promotes liquid-liquid phase separation of polyadenylation complexes. *Nature* **569**, 265–269
259. Vega, I. E., Umstead, A., and Kanaan, N. M. (2019) EFhd2 affects tau liquid-liquid phase separation. *Front. Neurosci.* **13**, 845
260. Ford, L. K., and Fioriti, L. (2020) Coiled-coil motifs of RNA-binding proteins: dynamics in RNA regulation. *Front. Cell Dev. Biol.* **8**, 607947
261. Lu, Y., Wu, T. T., Gutman, O., Lu, H. S., Zhou, Q., Henis, Y. I., et al. (2020) Phase separation of TAZ compartmentalizes the transcription machinery to promote gene expression. *Nat. Cell Biol.* **22**, 453–464

262. Rebane, A. A., Ziltener, P., LaMonica, L. C., Bauer, A. H., Zheng, H., Lopez-Montero, I., *et al.* (2020) Liquid-liquid phase separation of the Golgi matrix protein GM130. *FEBS Lett.* **594**, 1132–1144
263. Jiang, X. E., Ho, D. B. T., Mahe, K., Mia, J., Sepulveda, G., Antkowiak, M., *et al.* (2021) Condensation of pericentrin proteins in human cells illuminates phase separation in centrosome assembly. *J. Cell Sci.* **134**, jcs258897
264. Yan, W. X., Chen, G. H., and Li, J. C. (2022) Structure of the Harmonin PDZ2 and coiled-coil domains in a complex with CDHR2 tail and its implications. *FASEB J.* **36**, e22425
265. Ziltener, P., Rebane, A. A., Graham, M., Ernst, A. M., and Rothman, J. E. (2020) The golgin family exhibits a propensity to form condensates in living cells. *FEBS Lett.* **594**, 3086–3094
266. Lakadamali, M., Rust, M. J., and Zhuang, X. W. (2004) Endocytosis of influenza viruses. *Microbes Infect.* **6**, 929–936
267. Jahn, R., and Scheller, R. H. (2006) SNAREs - engines for membrane fusion. *Nat. Rev. Mol. Cell Biol.* **7**, 631–643
268. Sudhof, T. C., and Rothman, J. E. (2009) Membrane fusion: grappling with SNARE and SM proteins. *Science* **323**, 474–477
269. Yu, I. M., and Hughson, F. M. (2010) Tethering factors as organizers of intracellular vesicular traffic. *Annu. Rev. Cell Dev. Biol.* **26**, 137–156
270. Zhang, Y. L., and Hughson, F. M. (2021) Chaperoning SNARE folding and assembly. *Annu. Rev. Biochem.* **90**, 581–603
271. Mahendran, K. R., Niitsu, A., Kong, L. B., Thomson, A. R., Sessions, R. B., Woolfson, D. N., *et al.* (2017) A monodisperse transmembrane alpha-helical peptide barrel. *Nat. Chem.* **9**, 411–419
272. Verardi, R., Shi, L., Traaseth, N. J., Walsh, N., and Veglia, G. (2011) Structural topology of phospholamban pentamer in lipid bilayers by a hybrid solution and solid-state NMR method. *Proc. Natl. Acad. Sci. U. S. A.* **108**, 9101–9106
273. Hulkko, M., Berndt, F., Gruber, M., Linder, J. U., Truffault, V., Schultz, A., *et al.* (2006) The HAMP domain structure implies helix rotation in transmembrane signaling. *Cell* **126**, 929–940
274. McNamara, C., Zinkernagel, A. S., Macheboeuf, P., Cunningham, M. W., Nizet, V., and Ghosh, P. (2008) Coiled-coil irregularities and instabilities in group A Streptococcus M1 are required for virulence. *Science* **319**, 1405–1408
275. Kolesinski, P., Wang, K. C., Hirose, Y., Nizet, V., and Ghosh, P. (2022) An M protein coiled coil unfurls and exposes its hydrophobic core to capture LL-37. *Elife* **11**, e77989
276. Hagelueken, G., Clarke, B. R., Huang, H. X., Tuukkanen, A., Danciu, I., Svergun, D. I., *et al.* (2015) A coiled-coil domain acts as a molecular ruler to regulate O-antigen chain length in lipopolysaccharide. *Nat. Struct. Mol. Biol.* **22**, 50–56
277. Kammerer, R. A., Schulthess, T., Landwehr, R., Lustig, A., Engel, J., Aebi, U., *et al.* (1998) An autonomous folding unit mediates the assembly of two-stranded coiled coils. *Proc. Natl. Acad. Sci. U. S. A.* **95**, 13419–13424
278. Steinmetz, M. O., Stock, A., Schulthess, T., Landwehr, R., Lustig, A., Faix, J., *et al.* (1998) A distinct 14 residue site triggers coiled-coil formation in cortexillin I. *EMBO J.* **17**, 1883–1891
279. Burkhard, P., Kammerer, R. A., Steinmetz, M. O., Bourenkov, G. P., and Aebi, U. (2000) The coiled-coil trigger site of the rod domain of cortexillin I unveils a distinct network of interhelical and intrahelical salt bridges. *Structure* **8**, 223–230
280. Swanson, S., Sivaraman, V., Grigoryan, G., and Keating, A. E. (2022) Tertiary motifs as building blocks for the design of protein-binding peptides. *Protein Sci.* **31**, e4322
281. Merritt, H. I., Sawyer, N., and Arora, P. S. (2020) Bent into shape: folded peptides to mimic protein structure and modulate protein function. *Pept. Sci.* **112**, e24145
282. Lee, J. H., Kang, E., Lee, J., Kim, J., Lee, K. H., Han, J., *et al.* (2014) Protein grafting of p53TAD onto a leucine zipper scaffold generates a potent HDM dual inhibitor. *Nat. Commun.* **5**, 3814
283. Desmet, J., Verstraete, K., Bloch, Y., Lorent, E., Wen, Y., Devreese, B., *et al.* (2014) Structural basis of IL-23 antagonism by an Alphabody protein scaffold. *Nat. Commun.* **5**, 5237
284. Pannecouke, E., Van Trimpont, M., Desmet, J., Pieters, T., Reunes, L., Demoen, L., *et al.* (2021) Cell-penetrating Alphabody protein scaffolds for intracellular drug targeting. *Sci. Adv.* **7**, eabe1682
285. Kajava, A. V. (2012) Tandem repeats in proteins: from sequence to structure. *J. Struct. Biol.* **179**, 279–288
286. Pluckthun, A. (2015) Designed ankyrin repeat proteins (DARPins): binding proteins for research, diagnostics, and therapy. *Annu. Rev. Pharmacol.* **55**, 489–511
287. Gisdon, F. J., Kynast, J. P., Ayyildiz, M., Hine, A. V., Pluckthun, A., and Hocker, B. (2022) Modular peptide binders - development of a predictive technology as alternative for reagent antibodies. *Biol. Chem.* **403**, 535–543
288. Saudek, V., Pastore, A., Morelli, M. A. C., Frank, R., Gausepohl, H., and Gibson, T. (1991) The solution structure of a leucine-zipper motif peptide. *Protein Eng.* **4**, 519–529
289. Weis, W. I., Brunger, A. T., Skehel, J. J., and Wiley, D. C. (1990) Refinement of the influenza-virus hemagglutinin by simulated annealing. *J. Mol. Biol.* **212**, 737–761
290. Baker, E. G., Williams, C., Hudson, K. L., Bartlett, G. J., Heal, J. W., Goff, K. L. P., *et al.* (2017) Engineering protein stability with atomic precision in a monomeric miniprotein. *Nat. Chem. Biol.* **13**, 764–770
291. Sun, L., Young, L. N., Zhang, X. Z., Boudko, S. P., Fokine, A., Zbornik, E., *et al.* (2014) Icosahedral bacteriophage Phi X174 forms a tail for DNA transport during infection. *Nature* **505**, 432–435
292. Strelkov, S. V., Herrmann, H., Geisler, N., Wedig, T., Zimbelmann, R., Aebi, U., *et al.* (2002) Conserved segments 1A and 2B of the intermediate filament dimer: their atomic structures and role in filament assembly. *EMBO J.* **21**, 1255–1266